CXCL17 is an allosteric inhibitor of CXCR4 through a mechanism of action involving glycosaminoglycans

Carl W. White[1,2,3,5,6]*, Simon Platt[1,2], Laura E. Kilpatrick[2,4], Natasha Dale[3,5], Rekhati S. Abhayawardana[3,5] Sebastian Dekkers[1,2,4], Nicholas D Kindon[2,4], Barrie Kellam[2,4], Michael J Stocks[4], Kevin D. G. Pfleger[3,5,6]*, and Stephen J. Hill[1,2]*

1. Cell Signalling and Pharmacology Research Group, Division of Physiology, Pharmacology & Neuroscience, School of Life Sciences, University of Nottingham, Nottingham NG7 2UH, United Kingdom.

2. Centre of Membrane Proteins and Receptors, University of Birmingham and University of Nottingham, The Midlands, UK

3. Harry Perkins Institute of Medical Research and Centre for Medical Research, The University of Western Australia, QEII Medical Centre, Nedlands, Western Australia 6009, Australia

4. School of Pharmacy, Biodiscovery Institute, University of Nottingham, Nottingham NG7 2RD, United Kingdom.

5. Australian Research Council Centre for Personalised Therapeutics Technologies, Australia

6. Dimerix Limited, Melbourne, Australia

* Corresponding authors and persons to whom materials requests should be addressed:

stephen.hill@nottingham.ac.uk,

kevin.pfleger@uwa.edu.au

and/or carl.white@perkins.uwa.edu.au

Cell Signalling and Pharmacology Research Group,
School of Life Sciences, University of Nottingham
Queens Medical Centre
NG7 2UH, Nottingham, United Kingdom. Phone: +44-115-8230082

Editor's summary: CXCL17 GAGs a receptor

During inflammation, the orphan chemokine CXCL17, which is abundant in mucosal sites, aids in the recruitment of innate immune cells. White *et al*. sought to deorphanize CXCL17 by screening a panel of chemokine receptors for CXCL17 binding. CXCL17 allosterically inhibited ligand binding to and activation of the chemokine receptor CXCR4 in intact cells but did not affect the binding of CXCR4 to its agonist CXCL12 or its antagonists in dissociated membrane preparations. Disrupting putative glycosaminoglycan (GAG)-binding domains in CXCL17 reduced its interaction with and inhibition of CXCR4. Together, these findings suggest that CXCL17 acts as an endogenous inhibitor of CXCR4 signaling in a manner dependent on GAG-binding proteins.—Amy E. Baek

One-sentence summary: The chemokine CXCL17 may cooperate with glycosaminoglycan-containing proteins to inhibit the receptor CXCR4.

Abstract

CXCL17 is a chemokine principally expressed by mucosal tissues, where it facilitates chemotaxis of monocytes, dendritic cells, and macrophages and has antimicrobial properties. CXCL17 is also implicated in the pathology of inflammatory disorders and progression of several cancers, and its expression is increased during viral infections of the lung. However, the exact role of CXCL17 in health and disease requires further investigation, and there is a need for confirmed molecular targets mediating CXCL17 functional responses. Using a range of bioluminescence resonance energy transfer (BRET) based assays, here we demonstrated that CXCL17 inhibited CXCR4-mediated signalling and ligand binding. Moreover, CXCL17 interacted with neuropillin-1, a VEGFR2 co-receptor. Additionally, we found CXCL17 only inhibited CXCR4 ligand binding in intact cells and demonstrated that this effect was mimicked by known glycosaminoglycan binders, surfen and protamine sulfate. Disruption of putative GAG binding domains in CXCL17 prevented CXCR4 binding. This indicated that CXCL17 inhibited CXCR4 by a mechanism of action that potentially required the presence of a glycosaminoglycan containing accessory protein. Altogether, our results revealed that CXCL17 is an endogenous inhibitor of CXCR4 and represents the next step in our understanding of the function of CXCL17 and regulation of CXCR4 signalling.

Introduction

Chemokines are a large family of small, secreted cytokines that play a central role in the migration of cells. Chemokines are widely expressed throughout the body and facilitate both homeostatic as well as inflammatory immune responses. In addition, chemokines mediate numerous other physiological functions including angiogenesis and organogenesis as well as participate in pathophysiological processes such as cancer progression, autoimmune disorders, and aberrant inflammation[1]. Chemokines induce cellular responses by binding and activating G protein-coupled receptors (GPCRs). This results in the activation of heterotrimeric G proteins followed by downstream signalling, with subsequent β-arrestin recruitment to the chemokine receptor resulting in signal termination following receptor internalisation and desensitization[2].

CXCL17 is constitutively expressed at high levels in mucosal sites throughout the body and is thought to be involved in the innate immune response through the recruitment of monocytes, dendritic cells and macrophages[3,4]. In addition, CXCL17 has antimicrobial properties at high concentrations[5] and modulates angiogenesis[4,6]. CXCL17 has also been implicated in several pathologies including breast[7] and hepatocellular cancers[8], as well as inflammatory lung pathologies such as idiopathic pulmonary fibrosis[5], asthma[9], influenza[10] and SARS-CoV-2[11] infection. Despite mediating a wide range of important functional responses, the receptor(s) for CXCL17 are still unknown. Thus, it is vital to determine the molecular targets of CXCL17 not only to fully understand the normal function of CXCL17 but to allow targeting of its pathophysiological effects.

GPR35 has been implicated as the receptor for CXCL17[12], however other studies[13,14] have been unable to reproduce this finding to the best of our knowledge. Despite this, G protein-coupled receptors likely play a role in CXCL17-mediated signalling. Indeed, CXCL17-mediated calcium flux[12], inhibition of cAMP accumulation[15] and pertussis toxin sensitive signalling[4,16] have all been observed.

CXCR4 is a prototypical chemokine receptor that facilitates numerous physiological processes including organogenesis, hematopoiesis, and immune responses following activation by CXCL12. Moreover, CXCR4 signalling is involved in multiple diseases including various cancers, autoimmune disorders, aberrant inflammation and HIV-1 infection[17]. Therefore, the development of inhibitors of CXCR4 is an area of active research[18]. Notably, CXCL12 and CXCR4 are constitutively-expressed at high abundance widely throughout the body and several mechanisms exist to regulate CXCR4 signalling. These include: receptor oligomerisation; scavenging of CXCL12 by ACKR3 to decrease CXCL12 abundance; post-translational modifications; and proteolytic degradation of CXCL12[17]. Moreover, positively charged domains within CXCL12 mediate interactions with glycosaminoglycans that facilitate CXCL12 oligomerisation, prevent proteolytic degradation and help establish chemotactic gradients[19]. Finally, several endogenous inhibitors and modulators of CXCR4 have now been reported

including CXCL14[20], the endogenous cationic antimicrobial peptide cathelicidin LL37[21] a modulator of CXCR4 , as well as EPI-X4, an endogenous peptide fragment of serum albumin[22].

In this study, across a panel of chemokine receptors we found no agonist-like responses mediated by CXCL17. Instead, we showed that CXCL17 inhibited CXCR4-mediated signalling as well as ligand binding in intact live cells. CXCL17 was therefore an endogenous inhibitor of CXCR4. CXCL17 had no effect on binding of CXCL12, or a small molecule antagonist to CXCR4 in dissociated membrane preparations. This suggested that CXCL17 inhibited CXCR4 by a unique mechanism of action which we proposed involved an accessory protein containing glycosaminoglycans.

Results

GPR35 is not a direct target of CXCL17

In initial confirmatory experiments we sought to rule out GPR35 as a target for CXCL17 using bioluminescence resonance energy transfer (BRET) assays. In HEK293 cells transfected with GPR35/Nluc and β-arrestin2/Venus (fig S1A) the GPR35 agonist Zaprinast but not CXCL17 resulted in an increase in BRET indicative of recruitment of β-arrestin2/Venus to GPR35/Nluc confirming similar experiments published previously[13,14]. Similarly, in HEK293 cells transfected with GPR35, $G\alpha_{i1}$/Nluc and Venus/$G_{\gamma 2}$ (fig S1B), no change in the BRET ratio was observed with CXCL17 whereas Zaprinast decreased the BRET ratio in a GPR35 specific and concentration dependent manner (fig S2, pEC_{50} = 4.76 ± 0.82). Next, we examined whether GPR35 activation by CXCL17 required the co-expression of a chemokine receptor. Here HEK293 cells were transfected to co-express GPR35, $G\alpha_{i1}$/Nluc, Venus/$G_{\gamma 2}$ and a chemokine receptor (fig S1C). In each assay configuration the endogenous chemokine ligand resulted in a conformational change of the G protein complex (except for CCR9 for which no response was obtained with the positive control ligand) however CXCL17 at a concentration sufficient to induce signalling [6] produced no comparable or observable change in the BRET ratio. Taken together these data confirm GPR35 is not a direct target of CXCL17 under the tested experimental conditions.

CXCL17 inhibits CXCR4 signalling

Targets of CXCL17 are likely to be $G\alpha_i$ coupled G protein-coupled receptors due to reports of pertussis toxin sensitive signalling[4,16]. In HEK293 cells transfected with $G\alpha_{i1}$/Nluc, Venus/$G_{\gamma 2}$ and an individual chemokine receptor CCR1-10 or CXCR1-3, 5 or 6 (without co-expression of GPR35), endogenous chemokine ligands resulted in a decrease in the BRET ratio suggestive of receptor activation, however, no such change was observed using CXCL17 either in the absence or presence of a endogenous chemokine ligand (Fig 1A). In contrast, while CXCL17 did not induce an agonist-like response, we found that in HEK293 cells co-expressing CXCR4, $G\alpha_{i1}$/Nluc and Venus/$G_{\gamma 2}$, CXCL17 resulted in an increase in the BRET ratio as well as inhibited responses mediated by CXCL12 (Fig 1B) in a concentration-dependent manner (Fig 1C, pIC_{50} = 6.93 ± 0.28) albeit with a lower potency than the small molecule CXCR4 antagonist AMD3100 (pIC_{50} = 7.52 ± 0.03). CXCL17 had similar inhibitory effects in Cos-7 cells transiently transfected with CXCR4, $G\alpha_{i1}$/Nluc and Venus/$G_{\gamma 2}$, indicating these effects were not cell type dependent (fig S3). In addition, CXCL17 and the small molecule CXCR4 antagonist AMD3100 inhibited the CXCL12-mediated decrease in forskolin-induced cAMP accumulation (Fig 1D) in HEK293G cells that stably expressed the GloSensor cAMP biosensor and SNAP/CXCR4, which demonstrated that CXCL17 can inhibit downstream signalling. Altogether, these results suggest CXCL17 is a low potency selective inhibitor of CXCR4 signalling.

CXCL17 inhibits CXCR4-β-arrestin2 interactions

To confirm the inhibitory effects of CXCL17 we next investigated its effect on recruitment of β-arrestin-2 to the CXCR4. In HEK293 cells transfected with CXCR4/Rluc8 and β-arrestin2/Venus, application of CXCL17 (Fig 2A) resulted in a decrease in the basal BRET ratio as well as inhibition of CXCL12 mediated increases in BRET, thus indicating CXCL17 inhibits both constitutive and ligand-induced CXCR4 activity. The decrease in the basal BRET ratio following the application of CXCL17 was concentration-dependent (Fig 2B, pIC_{50} = 7.24 ± 0.08) and in HEK293 cells transfected with CXCR4/Nluc and β-arrestin2/Venus (Fig 2C) both CXCL17 (pIC_{50} = 6.85 ± 0.30) and AMD3100 (pIC_{50}= 7.79 ± 0.14) inhibited the increase in BRET mediated by CXCL12 in a concentration-dependent manner. To further test the specificity of CXCL17 for CXCR4, we used HEK293 cells transfected with CXCR1/Rluc8, CCR5/Rluc8 or β_2-adrenoceptor/Rluc8 (β_2-AR) and β-arrestin2/Venus. Each configuration showed an increase in BRET following application of a prototypical agonist but no modulation of the BRET ratio following application of CXCL17 (Fig 2D).

CXCL17 inhibits ligand binding to Nluc/CXCR4 in a context dependent manner

To examine binding of CXCL17 to CXCR4 we used a NanoBRET ligand binding approach. In live HEK293 cells stably-expressing exogenous CXCR4 tagged on the N-terminus with NanoLuc (Nluc/CXCR4), both AMD3100 and CXCL17 competed with CXCL12-AF647 (Fig 3A, pKi = 7.99 ± 0.16 and pKi = 6.25 ± 0.19 respectively) for Nluc/CXCR4 binding in a concentration-dependent manner. Previous studies demonstrate that the oligomeric state of CXCR4 is expression dependent and that oligomer formation and signalling can be disrupted by ligands such as IT1t that bind allosterically[23,24]. However, when binding experiments were performed in live HEK293 (fig S4A) or HeLa cells (fig S4b) CRISPR/Cas9 genome-edited to express Nluc/CXCR4 under endogenous promotion, and therefore with native levels of CXCR4 expression, AMD3100 (pKi = 8.01 ± 0.13 and pKi = 8.30 ± 0.08 respectively) and CXCL17 (pKi = 6.14 ± 0.30 and pKi = 6.15 ± 0.27 respectively) inhibited CXCL12-AF647 binding. These results rule out that this effect was specific to over-expressed CXCR4 receptors, potentially existing predominantly as CXCR4 oligomers, and further demonstrating inhibition was independent of cell type. Indeed, supporting a unique binding mode, CXCL17 did not compete with CXCL12-AF647 binding to Nluc/CXCR4 in membrane preparations from HEK293 cells stably-overexpressing the receptor (Fig 3B) whereas AMD3100 inhibited CXCL12-AF647 binding with an affinity similar to that observed in whole live cells (Fig 3B, pKi = 7.84 ± 0.06).

Differences in binding between whole cells and membranes could plausibly be due to internalisation and thus compartmentalisation of the receptor. In live HEK293 cells expressing SNAP/CXCR4, application of CXCL12 but not CXCL17 resulted in extensive receptor internalisation (Fig 3C).

Furthermore, using a Nanoluciferase complementation assay CXCL17 resulted in an increase in luminescence indicating accumulation of HiBiT/CXCR4 at the plasma membrane not internalisation (fig S5A). Additionally, when ligand binding was confined to the plasma membrane CXCL17 still resulted in the displacement of CXCL12-AF647 with similar affinity (fig S5B, pKi = 6.60 ± 0.1) in live cells even when agonist-induced internalisation and compartmentalisation was removed. Similarly, in permeabilised membrane preparations (Fig 3D), AMD3100 but not CXCL17 displaced CXCL12-AF647, ruling out that membrane vesicle formation was resulting in ligand-receptor compartmentalisation. Next, to investigate if more active forms of CXCL17 were being produced due to cleavage by cellular proteases in live cells, membrane preparations expressing Nluc/CXCR4 were co-incubated with wildtype HEK293 cells and binding investigated. However, no inhibition of CXCL12-AF647 binding by CXCL17 was observed (Fig 3E).

Finally, on close inspection of the competition ligand binding curves (Fig 3A and Fig 3B) we noted a steep slope >1 suggestive of non-competitive and/or allosteric interactions and therefore hypothesised CXCL17-mediated ligand displacement would be probe-dependent. To this end, the CXCR4 antagonists IT1t and AMD3100 (fig S6A) but not CXCL17 competed with binding of IT1t-BY630/650 (a fluorescent derivative of IT1t, fig S7A; with a $pK_d = 7.52 \pm 0.08$, fig S7B) to Nluc/CXCR4 expressed in live HEK293 cells (Fig 3F) or to Nluc/CXCR4 in membrane preparations (Fig 3G; pKi = 7.85 ± 0.07 and pKi = 8.51 ± 0.04 for IT1t in cells and membranes respectively). Structurally, the CXCR4 binding site(s) of CXCL12 only partially overlap with that of IT1t[25], which binds in a transmembrane region. The fact that CXCL17 only displaces binding of CXCL12 from CXCR4, and not the small molecule IT1t, suggests that while CXCL17 is interacting with CXCR4 the IT1t binding site is not targeted by CXCL17.

CXCL17 prevents endogenous CXCL12 binding to CXCR4

In our initial experiments we also noted that CXCL17 inhibits basal/constitutive CXCR4 signalling, suggesting inverse agonist activity. However, CXCL12 is endogenously expressed in the HEK293 cells used in these studies at levels sufficient to initiate signalling[26] and CXCR4 internalisation[27]. To investigate if CXCL17 was disrupting signalling mediated by endogenous CXCL12, we took advantage of HEK293 cells engineered using CRISPR/Cas9 genome-editing that express native CXCL12 tagged with HiBiT under endogenous promotion[26]. When the cells were transfected with exogenous SNAP/CXCR4, AMD3100 and CXCL17 both produced a concentration-dependent decrease in BRET (Fig 4, pIC_{50} = 7.10 ± 0.08 and 6.27 ± 0.16 respectively), generated between CXCL12-HiBiT and SNAP/CXCR4. These data support the ability of CXCL17 to inhibit CXCL12 binding to CXCR4 and indicate that inhibition of constitutive CXCR4 signalling is likely due to blocking endogenous CXCL12 binding to CXCR4.

Evidence for the involvement of glycosaminoglycans in CXCL17 inhibition of CXCR4

Chemokines, in addition to membrane receptors, bind GAGs through basic domains (putatively BBxB) that result in chemokine accumulation at the cell surface and facilitates oligomerisation as well as prevents proteolytic degradation. CXCL17 has an overall positive net charge of +18 at pH 7.4 and contains multiple highly conserved (fig S8) putative GAG domains (Fig 5A) indicating the potential to bind GAGs with high affinity. As generation of membrane preparations is likely to disrupt the extracellular matrix, we therefore hypothesised that CXCL17 required the presence of (unperturbed) membrane-bound glycosaminoglycans to inhibit CXCR4. To test this, we determined whether the effect of CXCL17 could be mimicked by known GAG binders. Both the small molecule GAG inhibitor surfen (Fig 5B) and the heparin antidote protamine sulfate (previously shown to inhibit CXCR4 signalling[28]; Fig 5C) inhibited CXCL12-AF647 binding to Nluc/CXCR4 in cells ($pK_i = 4.85 \pm 0.61$ and $pK_i = 6.35 \pm 0.13$ for surfen and protamine sulfate respectively) but neither surfen (Fig5D) or protamine sulfate (Fig 5E) altered binding in membranes. Further confirming that GAG binders can modulate CXCR4, surfen displaced CXCL12-HiBiT binding to SNAP/CXCR4 in live HEK293 cells in a concentration-dependent manner (Fig 4, $pIC_{50} = 5.07 \pm 0.12$). Consistent with the effects mediated by CXCL17, the slope of the concentration response curves of both GAG inhibitors was greater than 1 indicating an allosteric and/or non-competitive interaction. Notably, and as seen with CXCL17, surfen did not compete with IT1t-BY630/650 binding to Nluc/CXCR4 in live cells (fig S6A). Next, we used exogenous soluble heparan sulphate to pre-occupy the GAG binding sites of CXCL17 and therefore reduce its capacity to bind to endogenous GAG in the extracellular matrix. We observed that while heparan sulfate treatment had no effect on the binding of CXCL12 to Nluc/CXCR4 in live HEK293 cells (fig S6B), preincubation of CXCL17 with heparan sulfate reduced the ability of CXCL17 to displace CXCL12-AF647 binding from Nluc/CXCR4 but had no effect on AMD3100. Finally, we investigated if inhibition of CXCR4 ligand binding was a general property of high affinity GAG binders. Using a high concentration of CXCL4 (a.k.a. platelet factor 4, GAG affinity ~ 30 pM[29]) we did not observe inhibition of CXCL12-AF647 binding to Nluc/CXCR4 in live HEK293 cells (fig S6C). These results suggest GAGs are involved in the CXCL17 mediated inhibition and binding of CXCR4, but that not all known GAG binders can inhibit binding of CXCL12 to CXCR4.

To further investigate the ability of CXCL17 to bind GAGs, HEK293 cells were transfected with CXCL17 (Fig 6A) tagged with HiBiT. Fusion of HiBiT to the C-terminus of CXCL17 still inhibited CXCR4 mediated β-arrestin recruitment (fig S9A) and G-protein activation (fig S9B). However, treatment of cells with protamine sulfate, surfen or CXCL17 (Fig 6B) but not AMD3100 (Fig 6C, fig S10A) resulted in an increase in luminescence output following complementation of HiBiT with LgBiT. Binding of GAGs to HiBiT-tagged chemokines sterically hinders complementation of HiBiT with LgBiT [26]. The increase in luminescence is therefore consistent with GAG-bound CXCL17-HiBiT being

released into the assay medium due to being displaced by other GAG binders. Indeed, these effects were attenuated by pre-incubation of heparan sulfate with protamine sulfate or surfen (Fig 6B), which reduced the increase in luminescence. Notably, when cells were treated with heparin sulfate (Fig 6C, fig S10A) no additional formation of CXCL17-GAG complexes was evident as no change in luminescence was observed. This is in contrast to the effect of heparan sulfate on cells expressing CXCL12-HiBiT where it induces a large decrease in luminescence[26]. This indicates that unlike CXCL12 which is found both in a 'free' state and bound to GAGs[26], CXCL17 is largely bound to GAGs under basal conditions. Finally, when cells were treated with CXCL12 (Fig 6C, fig S10A) no change in luminescence was observed indicating a failure to displace CXCL17-GAG binding. In contrast CXCL17 (fig S10B) readily displaced binding of CXCL12-HiBiT to GAGs. Together this demonstrated that CXCL17 can interact with GAGs present in cultures of live cells with CXCL17 being strongly associated with GAGs under basal conditions.

Next to directly investigate CXCL17 binding to CXCR4, cells were transfected with both CXCL17-HiBiT and SNAP/CXCR4. As anticipated, we observed an increase in the BRET ratio. This demonstrated that CXCL17-HiBiT was indeed interacting in close proximity to SNAP/CXCR4 (Fig 6D). Moreover, protamine sulfate and surfen, but not AMD3100, resulted in a decrease in the BRET ratio supporting the involvement of GAGs in the binding of CXCL17 to CXCR4. However, no increase in BRET was observed when cells were transfected with CXCL17-HiBiT only or with SNAP/β_2-AR demonstrating that the increase in BRET ratio was not due to CXCL17 binding to the plasma membrane and producing a bystander BRET response (fig S10C).

The impact of a glycosaminoglycan binding-deficient mutant of CXCL17 on its binding to CXCR4.

To further understand the involvement of GAGs in the binding of CXCL17 to CXCR4 we mutated all basic residues in the key putative GAGs binding motifs (BBxB) in CXCL17 to alanine thus creating a GAG binding deficient CXCL17-HiBiT mutant (gag -ve CXCL17 HiBiT; Fig 6A). When HEK293 cells were transfected with equal amounts of wildtype CXCL17-HiBiT or mutant CXCL17-HiBiT we observed a marked 20-fold increase in luminescence output (Fig 6E) when the GAG binding sites had been mutated. This is consistent with an absence of GAG binding and consequent steric inhibition of HiBiT with LgBiT complementation that normally results in a decreased luminescence output. However, to confirm this observation we treated cells with protamine sulfate, surfen or CXCL17 with or without heparin sulfate (Fig 6B, Fig 6C, fig S10D). In contrast to wildtype CXCL17-HiBiT, no change in luminescence was observed following treatment with any compound indicating the mutant CXCL17-HiBiT lacked GAG binding ability. Finally, we tested the ability of the GAG binding deficient CXCL17-HiBiT mutant to interact with SNAP/CXCR4 in the NanoBRET binding assay. Again, in contrast to wildtype CXCL17, no increase in the BRET ratio over basal was observed in the absence or presence of protamine sulfate , surfen or CXCL17 (Fig 6D). Overall, the putative GAG binding

domains in CXCL17 are important for the binding of CXCL17 to GAGs and support bridge (Fig 6F) or GAG clustering (Fig 6G) interactions with CXCR4.

Binding of CXCL17 to the GAG-containing VEGFR2 co-receptor neuropilin-1.

While GAGs are important regulators of chemokine function *in vivo*, it is hypothesised that they are not strictly required for receptor binding. Indeed, dual GAG-receptor binding appears sterically unlikely for most chemokines[30]. In contrast, GAG binding motifs are required for ligand binding to some receptor tyrosine kinases[31]. Indeed, the vascular endothelial growth factor receptor 2 (VEGFR2) and its co-receptor neuropilin-1 (NRP1) both bind full length VEGF-A, however alternatively spliced isoforms of VEGF that lack a GAG binding motif do not bind to NRP1[32,33]. Using this model, we hypothesised that CXCL17 would only inhibit ligand-receptor binding where ligand-GAG interactions are a stringent requirement as is the case for binding to NRP1. Using NanoBRET ligand binding in HEK293 cells transfected with Nluc/VEGFR2 (Fig 7A), binding of a single site fluorescently-labeled version of VEGF ($VEGF_{165}$a-TMR[33,34]) that contains the putative GAG binding motif was displaced by unlabelled $VEGF_{165}$a, but not surfen, CXCL17 or CXCL12. In contrast in HEK293 cells transfected with Nluc/NRP1 (Fig 7B), $VEGF_{165}$a-TMR binding was displaced by unlabelled $VEGF_{165}$a, surfen and CXCL17 but not CXCL12. Finally, using cells transfected with CXCL17-HiBiT and SNAP/NRP1 we observed an increase in the BRET ratio demonstrating that CXCL17-HiBiT was binding to SNAP/NRP1. However, when protamine sulfate or surfen were present no increase in the BRET ratio was observed supporting the involvement of GAGs in the binding of CXCL17 to NRP1 (Fig 7C). Taken together, these results further support the involvement of GAG binding motifs in the binding mechanism of CXCL17 to cell surface receptors and suggests a direct interaction with VEGF signalling pathways.

Discussion

The first literature reports of CXCL17 show that CXCL17 has chemotactic properties for dendritic cells and monocytes[4], as well as correlating with VEGF expression[35]. Since then, our knowledge of CXCL17 in both health and disease has expanded to include functions such as being an important innate immune factor at mucosal barriers, as well as involvement in regulation of angiogenesis and tumorigenesis (for review see[36]). However, our current understanding is limited by a lack of *bonafide* molecular targets through which CXCL17 binds and elicits its function. GPR35, an orphan G protein-coupled receptor, is associated with the function of CXCL17. However, multiple investigations[13,14], including those presented here have failed to observe any similar CXCL17 mediated activation of GPR35

Here we reported an inhibitory interaction between CXCL17 and CXCR4 across multiple assays, cell lines and contexts. These results contrast with previous studies that observe no effect on CXCR4 signalling or ligand binding by CXCL17[6,12]. However, this is unsurprising given the fact that the focus of the previous investigations was on agonist-induced signalling (unlike the antagonistic responses seen here), and that previous ligand binding studies used membrane preparations which, as demonstrated in the current study, do not permit CXCL17 binding to CXCR4. *In vivo,* endogenous inhibition of CXCR4 function by enzymatic digestion or sequestration of CXCL12 represent important regulatory mechanisms to prevent excessive receptor activation. Here we observed that CXCL17 was approximately 10-fold less potent than the small molecule antagonists AMD3100 or IT1t in the functional assays tested. Therefore, making CXCL17 a relatively weak inhibitor of CXCR4 by comparison with synthetic antagonists. However, when compared to other endogenous CXCR4 inhibitors for example, CXCL14 K_d~14 nM[20] or EPI-X4 K_i~3 μM[22] CXCL17 has similar or high affinity for CXCR4. Notably CXCL17 concentrations can reach ~ 60 ng/ml in vitro while serum CXCL17 concentrations can reach ~ 5 ng/ml during influenza infection[10]. Since CXCL17 expression is highly localised to secretory cells in mucosal tissue[37] and the fact that CXCL17 binds to GAGs and is concentrated in the extracellular matrix in close proximity to the receptor, it is very likely that CXCL17 reaches local concentrations sufficient to inhibit CXCR4 and reduce signalling.

When compared to AMD3100, which is a weak partial CXCR4 agonist[38], and the inverse agonist IT1t[39], CXCL17 has a unique mechanism by which inhibition of CXCR4 is achieved. Here the most striking evidence for this that CXCL17 did not inhibit CXCL12-AF647 binding to CXCR4 in membrane preparations. We initially considered that a lack of CXCL17-mediated effects in membranes preparations was due to partitioning or internalisation of CXCR4 in cells. However, when ligand binding was limited to the plasma membrane using HiBiT-tagged CXCR4 or permeabilized cells, such a mechanism was not supported. CXCL17 therefore required intact cells to interact with or modulate the CXCL12 binding site on CXCR4 which supports the involvement of an accessory protein in the binding of CXCL17. In contrast to clear displacement of CXCL12 binding we found that CXCL17 did not displace a fluorescently-labeled derivative of IT1t from Nluc/CXCR4 in whole live cells or

membrane preparations. While initially surprising, this demonstrated that CXCL17 inhibits CXCR4 through a binding site that is different to that targeted by known small molecule inhibitors of CXCR4 such as IT1t and supports the concept that CXCL17 inhibits CXCR4 by a unique binding mechanism.

In our efforts to delineate the mechanism of action of CXCL17 we noted a steep slope >1 of CXCL17-mediated displacement of CXCL12-AF647 in the NanoBRET competition ligand binding curves which is indicative of an allosteric and/or non-competitive interaction. Furthermore, since CXCL17 had no effect in membrane preparations this suggested the involvement of a site that was lost once intact cells were disrupted and pointed to the involvement of an accessory protein. Here we present several lines of evidence that this potential accessory protein contained glycosaminoglycans: 1) CXCL17 contains multiple highly conserved putative GAG binding domains which when mutated prevented binding to GAGs as well as CXCR4; 2) Preparation of purified cell membranes likely disrupted the native structure, function and/or potentially presence of GAGs[40] thus preventing the ability of CXCL17 to bind to CXCR4; 3) the effect of CXCL17 was mimicked by known GAG binders, surfen and protamine sulphate; and 4) these known GAG binders displaced CXCL17-HiBiT binding from SNAP/CXCR4. Further evidence from the present study for the involvement of GAGs are: a) heparan sulfate reduced CXCL17-mediated inhibition of CXCL12-AF647 NLuc/CXCR4 binding presumably through the blockade of CXCL17 GAG binding domains and b) CXCL17 inhibited binding of $VEGF_{165}$a-TMR binding to NLuc/NRP1 but not NLuc/VEGFR2. This is notable as GAG binding domains are strictly required for $VEGF_{165}$a binding to NRP but not for binding to VEGFR2[33].

In addition, there does appear to be a level of specificity for CXCL17-mediated inhibition of CXCR4 since the high affinity GAG binder CXCL4[29] did not inhibit CXCR4, and CXCL17 did not broadly inhibit or activate other chemokine receptors. While yet to be determined, such specificity may be encoded through a dependence on the composition of the GAG side chains (for example, heparan sulfate versus chondroitin sulfate) for CXCL17 binding. Indeed, chemokine-GAG interactions are dependent on side chain preferences[41]. Alternatively, specificity may be through the need for CXCL17 to contain both GAG and CXCR4 binding domains, or inhibition of CXCR4 may depend on interactions with a specific membrane proteoglycan to bring specific GAG binding domains in close proximity with CXCR4. For example, in smooth muscle cells NRP1 is post-translationally modified by N-linked glycosylation and by the addition of *O*-linked chondroitin sulphate to serine 612 (S612) whilst in endothelial cells it is derivatised with heparan sulphate[42].

A plausible explanation for these results could be that CXCL17 participates in the release of an endogenous factor that subsequently binds and inhibits CXCR4. Indeed, competitive chemokine binding for GAGs induces cooperative signalling due to the 'release' of GAG bound chemokines subsequently activating a secondary receptor[43]. However, CXCL17 had no effect on CXCL12-CXCR4 interactions when membrane preparations expressing NLuc/CXCR4 were co-incubated with live intact wildtype HEK293 cells, making such an effect unlikely. In contrast, when considering the mechanism

of CXCL17 inhibition of CXCR4, these results principally support trans-interactions that are between CXCR4 and a proteoglycan/GAG on the same cell rather than cis interactions between receptors and GAGs on different cells. Thus, the simple presence of GAGs is not sufficient for CXCL17-mediated inhibition of CXCR4 and indicates that they also need to be in the correct orientation and/or close proximity.

It is notable for the interpretation of these results that CXCR4 forms complexes with membrane proteoglycans[44,45] and taken together this leads us to propose two potential modes of inhibition by CXCL17: 1) A 'bridge formation' where CXCL17 simultaneously binds to CXCR4 and a GAG in close proximity to the receptor (Fig 6F) or 2) a result of clustering of GAGs induced by CXCL17 in the vicinity of CXCR4 causing steric hindrance and reduced access of CXCL12 to the receptor (Fig 6G). In the first mechanism, elements of the GAG sidechain must contribute to the binding of CXCL17 to CXCR4. While we recognise that for most chemokines simultaneous binding to GAGs and chemokine receptors is unlikely due to the overlap of chemokine binding sites and/or steric hinderance[30], potential exceptions do exist; for example, for CCL21 and CXCL12γ that have extended C-terminal tails enriched in basic residues[19]. As the putative GAG binding domains of CXCL17 are positioned toward its C-terminus, similar to the situation with CCL21 and CXCL12γ, dual receptor-GAG binding may be structurally permitted. In support of option (2), reports demonstrate chemokines induce clustering of GAGs/proteoglycans[19]. Therefore, CXCL17-mediated clustering and stiffening of membrane proteoglycan complexes around CXCR4 could hinder the access of CXCL12 to the extracellular domains of CXCR4. This may also explain why CXCL17 did not interfere with the binding of a small molecule fluorescent derivative of IT1t, which binds within a transmembrane pocket of CXCR4[25] and due to its small size may more readily penetrate through clustered proteoglycans.

We note that formation of chemokine homodimers can modulate binding to their receptors. Moreover, the propensity for dimerization is chemokine dependent, can occur at a range of affinities, and dimer formation can be greatly enhanced by GAGs[41]. Here inhibition of CXCR4 was observed at concentrations of CXCL17 greater than 30 nM, with clear evidence for interactions with GAGs, which indicates the potential for dimer formation. CXCL17 oligomerisation is yet to be studied in detail. Therefore, future studies will need to establish if the molecular species binding to CXCR4 is a monomeric or dimeric form of CXCL17, as well as any involvement of GAGs in the formation of CXCL17 oligomers. This may yield further insight into the mechanism of CXCL17 binding to CXCR4.

While the exact mechanism of CXCL17-mediated inhibition requires further investigation, it is worth noting that the extracellular domains of CXCR4 are highly acidic and inhibition by highly basic peptides is a known phenomenon[46]. Positively charged CXCR4 inhibitors include the synthetic peptides TT22 (18-amino acids of which 8 are positively charged), ALX40-4C (nonapeptide of 9 arginines), T134 and T140 (argine/lysine rich peptides)[47] as well as the viral TAT protein[46] and the endogenous cationic antimicrobial peptide cathelicidin LL37 that can modulate CXCR4[21]. While here CXCL17 and the GAG

inhibitors protamine sulfate and surfen are all positively charged, the fact that inhibition of CXCR4 only occurs in intact cells indicates a unique mechanism of action that differentiates these molecules from those previously described. Further investigation of this mechanism may yield a novel approach to therapeutically target CXCR4.

CXCL17 has been reported to facilitate angiogenesis principally through secretion of pro-angiogenic factors such as VEGF-A and b-FGF[6,35]. Here binding of CXCL17 to NRP1 represents a direct interaction with the prototypical VEGF-A angiogenic pathway. NRP1 acts as a co-receptor that selectively potentiates VEGFR2 signaling, a key driver of angiogenesis, and has been reported to directly promote angiogenesis[32]. While we did not directly assess the effect on VEGF-A mediated signaling or angiogenesis, CXCL17-mediated angiogenesis by interactions with NRP1 is plausible and should be examined further. Furthermore, the potential for interplay between chemokines and receptor tyrosine kinases (RTKs) due to potential overlapping glycosaminoglycan binding is an intriguing finding, particularly since some RTKs require formation of an obligate RTK-GAG complex for ligand binding, for example FGF-2 binding to FGFR[48].

Previous studies report CXCL17 is a chemoattractant for dendritic cells, macrophages, and monocytes[3,4]. While we have not investigated such effects or other physiological functions here it is unlikely that CXCR4 or interactions with NRP-1 are driving CXCL17 mediated cell migration simply due to the inhibitory effects seen. This implies that further receptors for CXCL17 are still to be discovered. Moreover, here we have focused on the characterisation of the CXCL17-CXCR4 interaction rather than the role that CXCL17 may play in inhibiting the downstream responses of CXCR4 activation. Further investigation is therefore required to establish the receptors driving CXCL17 chemotaxis as well as the importance of CXCL17 modulation on physiological functions of CXCR4.

In summary, we demonstrated that CXCL17 inhibited CXCR4 and does so potentially through binding a glycosaminoglycan-containing accessory protein. These data suggest a unique mechanism of action that could be targeted to therapeutically inhibit CXCR4 in a cell type specific manner. Additionally, we confirmed that GPR35 does not play a role in the function of CXCL17 and furthermore demonstrated CXCL17 has the potential to modulate VEGF signalling pathways through direct interactions with the VEGFR2 co-receptor NRP1. Together, we identified CXCR4 and NRP1 as new molecular targets for CXCL17 which is a substantial contribution to our understanding of CXCL17 and may provide important insights into the patho/physiological roles of CXCL17.

Materials and Methods

Materials

AMD3100 was purchased from Selleckchem (USA) or Sigma-Aldrich (Australia). Unlabeled chemokine ligands were purchased from Preprotech (USA) except for 24Leu-CXCL17 which was purchased from R&D Systems. CXCL12-AF647 was purchased from Almac (United Kingdom). N,N'-Dicyclohexylcarbamimidothioic acid (5,6-dihydro-6,6-dimethylimidazo[2,1-b]thiazol-3-yl)methyl ester dihydrochloride (IT1t) was purchased from Tocris (United Kingdom). Bovine serum albumin, Isoprenaline, Forskolin, Heparan sulfate sodium salt, saponin, surfen hydrate, protamine sulfate and zaprinast were purchased from Sigma-Aldrich (Australia/United Kingdom). Furimazine, caged-furimazine (Endurazine), EnduRen, GloSensor cAMP reagent and purified LgBit NLuc fragments were from Promega Corporation (USA). SNAPTag AlexaFluor 488 membrane-impermeant substrate was from New England Biolabs. $VEGF_{165a}$ was purchased from R&D Systems and synthesis of fluorescent $VEGF_{165}$a-tetramethylrhodamine (TMR) has been described previously[34].

IT1t-BY630-650 ((6,6-Dimethyl-5,6-dihydroimidazo[2,1-b]thiazol-3-yl)methyl (E)-N-cyclohexyl-N'-((1r,4r)-4-(6-(2-(4-((E)-2-(5,5-difluoro-7-(thiophen-2-yl)-5H-4λ4,5λ4-dipyrrolo[1,2-c:2',1'-f][1,3,2]diazaborinin-3-yl)vinyl)phenoxy)acetamido)hexanamido)cyclo-hexyl)carbamimidothioate) was synthesised in the University of Nottingham. Purity of the compound was confirmed to be >95% by analytical HPLC. HRMS (ESI-TOF) calculated for $C_{50}H_{61}B_1F_2N_8O_3S_3$ $[M + H]^+$: 967.4168 found: 967.4238. Full synthetic details will be communicated shortly (manuscript in preparation).

AMD3100 was dissolved in water, unlabeled chemokines and CXCL12-AF647 were dissolved as per the manufacturer's instructions. $VEGF_{165}$a was dissolved in phosphate buffered saline (PBS) containing 0.1% bovine serum albumin (BSA; Sigma Aldrich). IT1t and Zaprinast were dissolved in DMSO to a concentration of 10 mM. All further dilutions were performed in assay buffer containing 0.1% BSA.

Molecular biology and construct sources

Expression cDNA constructs encoding untagged chemokine receptors, β_2-adrenoceptor or GPR35 were purchased from the cDNA Resource Center. To generate the pcDNA3.1 mammalian expression vector encoding for CXCL17-HiBiT, DNA was synthesized by IDT and sub-cloned into the vector using the restriction enzymes HindIII and XbaI. To generate pcDNA3.1 vector encoding a GAG binding deficient mutant of CXCL17, HiBiT DNA was synthesised by Genescript into a pcDNA 3.1 vector. The putative GAG binding domains were mutated to alanine in CXCL17. Mutated amino acids in the GAG binding deficient mutant are H32A, R33A, R35A, K85A, K86A, R88A, R91A, H92A, R94A, K98A, H99A and R101A. See Table S1 for full DNA sequences of wildtype and mutant CXCL17-HiBiT and Fig 6A for protein sequences. To generate the pcDNA3.1(+) mammalian expression vector encoding for GPR35 tagged on the C-terminus with NLuc, the stop codon was first removed by site directed mutagenesis.

The primers used were forward 5'-CCTCTAGACTCGAGTGCGGCGAGGGTCACGCA-3' and reverse 5'-TGCGTGACCCTCGCCGCACTCGAGTCTAGAGG-3'. Nluc was then sub-cloned into the vector from existing constructs using the restriction enzymes XhoI and ApaI. Generation of pcDNA3.1 (+) neo expression constructs encoding NLuc/CXCR4, HiBiT/CXCR4[27], SNAP/β2AR[49], SNAP/CXCR4[26], NLuc/VEGFR2[34], NLuc/NRP[33] and SNAP/NRP[33] have been described previously, as have pcDNA3 expression constructs encoding CXCR4/Rluc8[50], CXCR4/Nluc[51], β-arrestin2/Venus[52]. Venus/Gγ2 was a kind gift from Dr. Martina Kocan. $G\alpha_{i1}$/NLuc was generated from the $G\alpha_{i1}$/Rluc8 construct reported previously[53].

Cell culture

HEK293F/T (Life Technologies, R70007), HEK293G (gift from Promega, HEK293 cells, RRID:CVCL_0045, stably expressing the GloSensor cAMP biosensor), HeLa (gift from Steve Briddon, University of Nottingham, RRID:CVCL_0030) and Cos-7 (ATCC, RRID:CVCL_0224) cells were maintained in Dulbecco's Modified Eagle's Medium (Sigma Aldrich or Thermo Fisher Scientific) supplemented with 10 % fetal calf serum at 37°C/5% CO_2. Stable transfections were performed using FuGENE (Promega, USA) according to the manufacturer's instructions. Cells were not routinely tested for contaminants. Generation of HEK293 cell lines stably-expressing Nluc/CXCR4, HiBiT/CXCR4 or SNAP/CXCR4, or generation of HEK293 or HeLa cells that were genome-edited to express NLuc/CXCR4 or CXCL12-HiBiT under endogenous promotion, have been described previously[26,27]. To generate cells for use in the GloSensor cAMP assay, HEK293G cells stably-expressing the GloSensor cAMP biosensor were transfected with a pcDNA3.1 (+) neo expression vector encoding SNAP/CXCR4 and subsequently selected for incorporation of the transgene using G418 (ThermoFisher).

BRET β-arrestin2 recruitment assays

HEK293F/T cells were maintained in DMEM containing 0.3 mg/ml glutamine, 100 IU/ml penicillin and 100 µg/ml streptomycin supplemented with 10% FBS (Bovogen) and 400-µg/mL geneticin. Cells were harvested when cells reached 70-80% confluency using phosphate-buffered saline (PBS) and 0.05% trypsin-EDTA and seeded in a 6 well plate at 300,000 cells/well. 24 hours later cells were transiently transfected with pcDNA3 mammalian expression vectors encoding CXCR4/Rluc8 (100 ng per well) and β-arrestin2/Venus (300 ng per well) using FuGENE and incubated at 37°C/5% CO_2 for 24 h. Cells were harvested into white 96-well plates at 100,000 cells/well in phenol-red free DMEM containing 25 mM HEPES, 0.3 mg/ml glutamine, 100 IU/ml penicillin and 100 µg/ml streptomycin supplemented with 5% FCS (phenol-red free DMEM) and incubated at 37°C/5% CO_2 for 24 h. On the day of assay, culture medium was removed and cells incubated with EnduRen (30 µM) in pre-warmed Hanks-buffered saline solution without calcium or magnesium (Hanks buffer, Thermo Fisher Scientific)

for 2 hours at 37 °C. Real-time BRET measurements were taken at 37 °C using a LUMIstar (BMG Labtech). In all experiments, initial measurements were taken to establish the baseline BRET ratio before CXCL12 (10 nM) or CXCL17 (1 pM – 1 μM) was added to the cells. In a subset of experiments, vehicle or CXCL12 (10 nM) was added and the BRET allowed to plateau before CXCL17 (100 nM) was added to the cells. Filtered light emissions were sequentially measured at 475 nm (30 nm bandpass) and 535 nm (30 nm bandpass) in triplicate wells. The corrected BRET signal was calculated by subtracting the ratio of the acceptor 535/30 nm emission over the donor 475/30 nm emission for a vehicle-treated cell sample from the same ratio for a sample treated with agonist. In this calculation, the vehicle-treated cell sample represents the background, eliminating the requirement for measuring a donor-only control sample. Points represent the maximal change in the BRET ratio following ligand addition from the kinetic read. In a subset of experiments, HEK293 cells where transfected with cDNA encoding CXCR1/RLuc8, CCR5/RLuc8 or β_2-adrenoceptor/RLuc8 (100 ng per well) and β-arrestin2/Venus (300 ng per well), and following establishment of the baseline BRET ratio, cells were incubated with either CXCL17 (300 nM) or CXCL8 (10 nM), CCL5 (10 nM) or Isoprenaline (100 μM) respectively.

To investigate β-arrestin/Venus recruitment to GPR35/NLuc, 300,000 cells in a 6 well plate were transfected with pcDNA3 mammalian expression vectors encoding GPR35/NLuc (25 ng per well) and β-arrestin2/Venus (300 ng per well), then seeded at 30,000 cells/well in a 96 well plate 24 hours later. On the day of assay, cells were washed and incubated with Hanks buffer for 1 hour at 37 °C before furimazine (10 μM) was added. Cells were incubated for a further 5 mins at 37 °C before real-time BRET measurements were taken at 37 °C using a LUMIstar as described above. Following establishment of the baseline BRET ratio, cells were treated with vehicle or CXCL17 (100 nM) or Zaprinast (100 μM).

To establish the pIC_{50} of CXCL17 in Fig 2C, HEK293 cells were maintained in Dulbecco's Modified Eagle's Medium (Sigma Aldrich) supplemented with 10 % fetal calf serum at 37°C/5% CO_2. Cells were passaged or harvested when cells reached 70-80% confluency using Phosphate-Buffered Saline (PBS, Sigma Aldrich) and trypsin (0.25% w/v in versene; Sigma Aldrich). Cells were seeded at 300,000 cells/well in a 6 well plate and incubated for 24h at 37°C/5%CO_2 before being transfected with CxCR4/NLuc (25 ng per well) and β-arrestin2/Venus (300 ng per well) using FuGENE. Cells were seeded into poly-D-lysine coated white flat bottom 96 well plates at 40,000 cells/well and incubated for 24h at 37°C/5% CO_2. On the day of the assay, cells were washed and incubated with pre-warmed HEPES-Buffered Salt Solution (HBSS; 25mM HEPES, 10mM glucose, 146mM NaCl, 5mM KCl, 1mM $MgSO_4$, 2mM sodium pyruvate, 1.3mM $CaCl_2$, 1.8g/L glucose; pH 7.2) supplemented with 0.1% BSA containing CXCL17 (0.3 nM – 1 μM) or AMD3100 (10 pM – 300 nM) for 1 hour at 37°C. Following incubation with furimazine (10 μM) for 5 minutes before sequential filtered light emissions were taken using a PHERAStar FS plate reader (BMG Labtech) using 475 nm (30 nm bandpass) and 535 nm (30

nm bandpass) filters in duplicate wells. Following establishment of the baseline BRET ratio, vehicle or CXCL12 (10 nM) was added to the cells before further filtered light emissions were taken. The corrected BRET signal was calculated by subtracting the ratio of the acceptor 535/30 nm emission over the donor 475/30 nm emission for a vehicle-treated cell sample from the same ratio for a sample treated with agonist.

G protein activation assays

HEK293 or Cos-7 cells were maintained in DMEM containing 0.3 mg/ml glutamine, 100 IU/ml penicillin and 100 µg/ml streptomycin supplemented with 10% FBS (Bovogen) and 400-µg/mL geneticin. Cells were seeded in a 6 well plate at 300,000 cells/well and 24 hours later cells were transiently transfected with pcDNA3 mammalian expression vectors encoding $G\alpha_{i1}$/Nluc (50 ng/well) and Venus/$G_{\gamma 2}$ (100 ng/well) as well as empty pcDNA3 or GPR35 (50 ng/well) with or without cDNA encoding a chemokine receptor (CCR1-CCR10 or CXCR1-CXCR6, 125 ng/well) or alternatively cells were transfected with $G\alpha_{i1}$/Nluc (50 ng/well), Venus/$G_{\gamma 2}$ (100 ng/well) as well as chemokine receptor (CCR1-CCR10 or CXCR1-CXCR6, 100 ng/well) using FuGENE and incubated at 37°C/5% CO_2 for 24 h. Cells were then harvested and were seeded into poly-L-lysine coated white flat bottom 96 well plates in phenol-red free DMEM at 50,000 cells/well and incubated for 24h at 37°C/5% CO_2. On the day of the assay, medium was aspirated, and the cells were incubated with pre-warmed Hanks buffer supplemented with 0.1% BSA containing Endurazine (10 µM) for 2 hours at 37°C. Sequential filtered light emissions were then recorded using a LUMIstar plate reader using 475 nm (30 nm bandpass) and 535 nm (30 nm bandpass) filters to establish a baseline BRET ratio. Cells were then treated with ligands and the BRET ratio continuously monitored. In assays investigating GPR35 only, triplicate wells were treated with Zaprinast (100 µM, or 10 nM – 300 µM for concentration response curves) or CXCL17 (100 nM) duplicate wells. Where GPR35 and a chemokine receptor were co-expressed, cells were stimulated with CXCL17 (30 nM) in duplicate wells or 30 nM of CCL3, CCL2, CCL13, CCL22, CCL4, CCL20, CCL19, CCL1, CCL25, CCL27, CXCL8, CXCL8, CXCL11, CXCL12, CXCL13 and CXCL16 in triplicate wells for CCR1-CCR10 and CXCR1-6 respectively. Triplicate wells of HEK293 cells expressing CXCR4 were treated with CXCL12 (1 nM), CXCL17 (300 nM), or CXCL12 (1 nM) and CXCL17 (300 nM). Cos-7 cells expressing CXCR4 were treated in triplicate with CXCL12 (10 nM), CXCL17 (300 nM) or CXCL12 (10 nM) and CXCL17 (300 nM). In HEK293 cells where CCR1-CCR10 and CXCR1-3, 5 and 6 were expressed, duplicate wells of cells were treated with CXCL17 (300 nM) or a submaximal concentration of chemokine CCL3 (0.3 nM), CCL2 (0.3 nM), CCL13 (1 nM), CCL22 (0.3 nM), CCL4 (30 nM), CCL20 (3 nM), CCL19 (1 nM), CCL1 (10 nM), CCL25 (10 nM), CCL27 (10 nM), CXCL8 (0.3 nM), CXCL8 (1 nM), CXCL11 (1 nM), CXCL13 (3 nM) and CXCL16 (1 nM) for CCR1-10 and CXCR1-3, 5 and 6 respectively in the absence or presence of CXCL17 (300 nM). In these experiments' cells were preincubated with CXCL17 for 15 mins prior to establishing the baseline

BRET ratio. Corrected BRET ratios were calculated by subtracting the ratio of the 535 nm emission (acceptor) by the 475 nm emission (donor) for a vehicle-treated cell sample from the same ratio for a sample treated with agonist. For concentration-response curves or bar graphs, data represent the maximal change in the corrected BRET ratio.

To establish the pIC_{50} of CXCL17 in Fig 1C, HEK293 cells were maintained in Dulbecco's Modified Eagle's Medium (Sigma Aldrich) supplemented with 10% fetal calf serum at 37°C/5% CO_2. Cells were harvested when they reached 70-80% confluency using Phosphate Buffered Saline (PBS, Sigma Aldrich) and trypsin (0.25% w/v in versene; Sigma Aldrich) and seeded at 300,000 cells/well in a 6 well plate and incubated for 24h at 37°C/5% CO_2 before being transfected with CXCR4 (10 ng per well), $G\alpha_{i1}$/Nluc (50 ng/well) and Venus/$G_{\gamma 2}$ (100 ng/well) using FuGENE. 24 hours later, cells were harvested and seeded into poly-D-lysine coated white flat bottom 96 well plates at 40,000 cells/well and incubated for 24h at 37°C/5% CO_2. On the day of the assay, cells were washed and incubated with pre-warmed HBSS supplemented with 0.1% BSA containing CXCL17 (0.3 nM – 1 μM) or AMD3100 (10 pM – 300 nM) for 30 minutes at 37°C. Cells were then incubated with furimazine (10 μM) for 10 minutes before filtered light emissions were taken using a PHERAStar FS plate reader using 475 nm (30 nm bandpass) and 535 nm (30 nm bandpass) filters in duplicate wells. Following establishment of the baseline BRET ratio, vehicle or CXCL12 (0.1 nM) was added to the cells before further filtered light emissions were taken. The corrected BRET signal was calculated by subtracting the ratio of the acceptor 535/30 nm emission over the donor 475/30 nm emission for a vehicle-treated cell sample from the same ratio for a sample treated with agonist.

GloSensor cAMP assay

GloSensor cAMP assay was performed according to the manufacturer's instructions. Briefly, HEK293G cells stably expressing SNAP/CXCR4 were seeded into poly-D-lysine coated white flat bottom 96 well plates at 30,000 cells/well and incubated for 24h at 37°C/5% CO_2. On the day of the assay, cells were washed then incubated with pre-warmed HBSS containing 6% GloSensor cAMP reagent and 0.1% BSA for 1.5 hours at 37°C. Cells in duplicate wells were then pre-incubated with or without AMD3100 (1μM) or CXCL17 (1 μM) for 30 minutes before total light emissions were measured on a PHERAStar FS plate reader to establish baseline luminescence. Forskolin (30 μM) in the absence or presence of CXCL12 (1 nM) was then added and total luminescence measured for a further 1 hour. Data represents % of the forskolin (30 μM) mediated cAMP production and was calculated from the area under the curve following ligand addition.

NanoBRET ligand binding assays

HEK293T cells stably expressing NLuc/CXCR4, HiBiT/CXCR4 or HEK293F/T as well as HeLa cells expressing genome-edited NLuc/CXCR4 were maintained in Dulbecco's Modified Eagle's Medium (Sigma Aldrich) supplemented with 10% fetal calf serum at 37°C/5% CO_2. Cells were passaged or harvested when they reached 70-80% confluency using Phosphate Buffered Saline (PBS, Sigma Aldrich) and trypsin (0.25% w/v in versene; Sigma Aldrich). Membrane preparations expressing genome-edited or stably-expressed NLuc/CXCR4 were made as described previously[54].

For competition binding experiments, cells expressing NLuc/CXCR4 were seeded into poly-D-lysine coated white flat bottom 96 well plates at 30,000 cells/well and incubated for 24h at 37°C/5% CO_2. On the day of the assay, cells were washed and incubated with pre-warmed HBSS supplemented with 0.1% BSA. For assays using membrane preparations expressing NLuc/CXCR4 from genome-edited or stably transfected HEK293 cells, 10 μg membrane protein diluted in HBSS supplemented with 0.1% BSA was loaded into each well. Cells or membranes were then incubated with CXCL12-AF647 (12.5 nM) or IT1t-BY630/650 (100 nM) in the absence or presence of AMD3100 (1 pM – 10 μM), CXCL4 (1 μM), CXCL12 (0.1 pM – 1 μM), CXCL17 (1pM – 1 μM), IT1t (1 pM – 10 μM), Surfen (10 pM – 10 μM) or protamine sulfate (1nM – 10 μM) for 1 hour at 37°C. All experiments in membranes and cells were performed in triplicate and duplicate wells respectively. All experiments testing an unknown inhibitor of CXCR4 (CXCL17, Surfen or Protamine sulfate) where performed with a known CXCR4 ligand (AMD3100, CXCL12, IT1t) as a control. Following incubation, furimazine (10 μM) was added and plates equilibrated for 5 minutes at room temperature before sequential filtered light emissions were taken using a PHERAStar FS plate reader using 460nm (80nm bandpass) and >610nm (longpass) filters. BRET ratios were calculated by dividing the 610nm emission (acceptor) by the 460nm emission (donor). For cells expressing HiBiT/CXCR4, experiments were performed as described above in duplicate wells but following ligand incubation both furimazine (10 μM) and purified LgBiT (10 nM) were added to generate luminescence. This allowed ligand binding to be confined the plasma membrane due to the cell impermeant nature of the purified LgBiT fragment of NanoLuc.

In subsets of experiments the NanoBRET competition binding assays were performed as described above but with the following modifications: In Fig 3D, to determine the effect of membrane permeabilization with saponin, 10 μg membrane protein diluted in HBSS supplemented with 0.1% BSA was loaded into duplicate wells each containing 0.25 mg/mL saponin and membranes incubated with CXCL12-AF647 (12.5 nM) in the absence or presence of AMD3100 (1 μM) or CXCL17 (300 nM) for 1 hour at 37°C. In Fig 3E, to determine if cellular proteases were required to convert CXCL17 into a more active species, wildtype HEK293 cells were seeded into poly-D-lysine coated white flat bottom 96 well plates at 30,000 cells/well and incubated for 24h at 37°C/5% CO_2. On the day of the assay, cells were washed and 10 μg membrane protein diluted in HBSS supplemented with 0.1% BSA loaded into duplicate wells containing cells and incubated with CXCL12-AF647 (12.5 nM) in the absence or

presence of increasing concentrations of AMD3100 (1 pM – 10 μM) or CXCL17 (100 pM – 1 μM), for 1 hour at 37°C. In fig S6B, to investigate the effect of exogenous heparan sulfate on CXCL17, on the day of the assay HEK293 cells expressing NLuc/CXCR4 were washed and incubated with pre-warmed HBSS supplemented with 0.1% BSA before AMD3100 (1 μM) or CXCL17 (300 nM) that had been preincubated with or without heparan sulfate (30 μg/ml) for 1 hour was added to duplicate wells of cells. CXCL12-AF647 (12.5 nM) was then added to each well and incubated for 30 mins at 37°C before the plate was read.

For competition binding experiments expressing NLuc/VEGFR2 or NLuc/NRP1, wildtype HEK293 cells were seeded into poly-D-lysine coated white flat bottom 96 well plates at 10,000 cells/well and incubated for 24h at 37°C/5% CO_2. Cells were then transiently transfected with 100 ng/well cDNA encoding NLuc/NRP1 or NLuc/VEGFR2 using FuGENE (Promega, USA) according to the manufacturer's instructions and incubated for a further 24h at 37°C/5% CO_2. On the day of the assay, cells were washed and incubated with pre-warmed HBSS supplemented with 0.1% BSA. Duplicate wells of cells were then incubated with $VEGF_{165}$a-TMR (3 nM) in the absence or presence of CXCL12 (1 μM), CXCL17 (300 nM), Surfen (30 μM) or $VEGF_{165}$a (30 μM) for 1 hour at 37°C. Following incubation, furimazine (10 μM) was added and plates equilibrated for 5 minutes at room temperature before sequential filtered light emissions were measured using a PHERAStar FS plate reader using 460nm (80nm bandpass) and >610nm (longpass) filters. BRET ratios were calculated by dividing the 610nm emission (acceptor) by the 460nm emission (donor).

Determination of IT1t-BY630-650 affinity by NanoBRET saturation ligand binding

Genome-edited cells expressing NLuc/CXCR4 were seeded into poly-D-lysine coated white flat bottom 96 well plates at 30,000 cells/well and incubated for 24h at 37°C/5% CO_2. On the day of the assay, duplicate wells of cells were washed and incubated with pre-warmed HBSS supplemented with 0.1% BSA and incubated with increasing concentrations of IT1t-BY630/650 in the absence or presence of IT1t (10 μM) for 1 hour at 37°C. Furimazine (10 μM) was added, and plates equilibrated for 5 minutes at room temperature before sequential filtered light emissions were taken using a PHERAStar FS plate reader using 460nm (80nm bandpass) and >610nm (longpass) filters. BRET ratios were calculated by dividing the 610nm emission (acceptor) by the 460nm emission (donor).

Nano luciferase complementation internalisation assays

HEK293 cells stably expressing HiBiT/CXCR4 were seeded into poly-D-lysine coated white flat bottom 96 well plates at 30,000 cells/well and incubated for 24h at 37°C/5% CO_2. On the day of the assay, duplicate wells of cells were washed and incubated with pre-warmed HBSS supplemented with 0.1% BSA. A concentration-response curve was generated by incubating cells with CXCL17 (10 pM –

1 uM) for 60 minutes at 37°C. Following ligand incubation, furimazine (10 μM) and purified LgBiT (10 nM) were added and plates incubated for 5 minutes before total light emissions were continuously measured using a PHERAStar FS plate reader with the concentration-response curves representing the luminescence after 30 minutes.

Assessment of internalisation by fluorescent microscopy

HEK293G cells stably expressing SNAP/CXCR4 were seeded into poly-D-lysine coated 8-well plates at 10,000 cells/well and incubated for 24h at 37°C/5% CO_2. On the day of the assay, cells were incubated with 0.5 μM membrane impermeant SNAP-tag AF488 for 30 minutes at 37°C/5% CO_2 prepared in serum-free DMEM. Cells were then washed three times with HBSS/0.1% BSA and incubated with CXCL12 (100 nM), CXCL17 (300 nM) or vehicle (HBSS/0.1% BSA) for 1 hour in the dark at 37°C. Cells were imaged live at 37°C using a Zeiss LSM710 fitted with a 63x Plan Apochromat oil objective (1.4NA) using a Argon488 (AlexaFluor488; 496-574nm band pass; 2% power) with a 488/561/633 beamsplitter using a pinhole diameter of 1 Airy unit. All images were taken at 1024x1024 pixels per frame with 8 averages (zoom 1).

CXCL12-HiBiT NanoBRET competition ligand binding assays

HEK293 cells expressing genome-edited CXCL12-HiBiT were seeded in 6 well plates at 300,000 cells per well and incubated for 24h at 37°C/5% CO_2. Cells were then transfected with 500 ng/well pcDNA3.1 (neo) plasmid encoding SNAP/CXCR4 and incubated for a further 24h before seeding into poly-D-lysine coated white flat bottom 96 well plates at 60,000 cells/well and incubated for 24h at 37°C/5% CO_2. On the day of the assay, duplicate wells of cells were incubated with 0.25 μM membrane impermeant SNAP-tag AF488 for 1h at 37°C/5% CO_2 prepared in serum-free DMEM. After incubation, cells were washed 3 times with pre-warmed HBSS supplemented with 0.1% BSA and incubated with purified 30 nM purified LgBiT in the absence or presence of AMD3100 (1 pM – 10 μM), Surfen (3 nM – 30 μM) or CXCL17 (100 pM – 1 μM) for 2h at 37°C. Following ligand incubation, 10 μM furimazine was added and plates equilibrated for 5 mins at room temperature. To determine basal BRET, SNAP-tagAF488 was omitted during labelling. Sequential filtered light emissions were recorded using a PHERAStar FS plate reader using 475 nm (30 nm bandpass) and 535 nm (30 nm bandpass) filters. BRET ratios were calculated by dividing the 535 nm emission (acceptor) by the 475 nm emission (donor).

CXCL17 HiBiT secretion assays

To investigate the effect of the disruption of putative CXCL17 GAG binding domains on CXCL17 release into culture media, plasmids were generated with the putative BBxB GAG domains in CXCL17 replaced with an alanine. HEK293T cells were seeded in 6 well plates at a density of 300,000 cells/well. Twenty four hours later cells were transfected with plasmids encoding CXCL17-HiBiT or gag -ve

CXCL17-HiBiT (both in pCDNA3.1, 250 ng DNA/well using FuGeneHD at a 3:1 ratio µl:µg according to manufacturer's instructions) and incubated for a further 24 hours. Subsequently cells were dissociated and seeded into Poly-D-Lysine coated white 96 well plates at a density of 40,000 cells per well and cultured for a further 24 hours. To perform the assay, culture media was removed, and duplicate wells of cells incubated for two hours in HBSS + 0.1% BSA containing 30 nM LgBiT at 37 °C, 0% CO_2. Following addition of furimazine (1:40 final concentration) luminescence was recorded using a PheraStar plate reader (BMG Labtech), using the LUM Plus setting. Following 10 minutes of baseline monitoring, the plate was removed, and treatments added at the final concentrations: Surfen (10 µM), Protamine sulfate (1 µM), CXCL17 (100 nM), AMD3100 (1 µM), CXCL12 (100 nM), Heparan sulfate (30 µg/ml), Surfen (10 µM) + Heparan Sulfate (30 µg/ml), Protamine Sulfate (1 µM) + Heparan Sulfate (30 µg/ml), or vehicle, and luminescence monitored for a further 50 minutes. Baseline luminescence was reported in relative luminescence units, and luminescence following drug treatment expressed as a percentage of baseline luminescence. In a subset of experiments the effect of CXCL17 (300 nM) on secretion and GAG binding of CXCL12-HiBiT was investigated. These experiments were performed as described previously[26].

CXCL17 HiBiT NanoBRET binding assays

To investigate the effect of the disruption of putative CXCL17 GAG domains on CXCL17 – CXCR4 interaction, NanoBRET assays were performed in live cells. HEK293T cells were seeded in 6 well plates at a density of 300,000 cells/well. Twenty four hours later cells were transfected with plasmids encoding SNAP/CXCR4 (500 ng) in combination with either CXCL17-HiBiT or gag -ve CXCL17-HiBiT (both in PCDNA3.1, 500 ng DNA/well) using FuGeneHD at a 3:1 ratio µl:µg according to manufacturer's instructions, and incubated for a further 24 hours. Cells were seeded into white 96 well plates at a density of 40,000 cell per well and incubated for 24 hours. Prior to the assay, triplicate wells of cells were incubated in serum free media containing 250 nM SNAP-Surface Alexa Fluor 488 substrate for 1 hour at 37 °C. For no acceptor controls, the SNAP-Surface Alexa Fluor 488 substrate was omitted. Cells were then washed twice with HBSS + 0.1% BSA and incubated with HBSS + 0.1% BSA containing 30 nM LgBiT, and Surfen (10 µM), Protamine sulfate (1 µM), AMD3100 (1 µM), or vehicle, for two hours. Cells were then supplemented with Furimazine (1:40 final concentration) and sequential filtered light emissions were recorded using a PHERAStar FS plate reader using 475 nm (30 nm bandpass) and 535 nm (30 nm bandpass) filters. BRET ratios were calculated by dividing the 535 nm emission (acceptor) by the 475 nm emission (donor).

In a subset of experiments, specificity of CXCL17-HiBiT binding was investigated, HEK293 cells stably expressing CXCL17-HiBiT were seeded in 6 well plates at 300,000 cells per well and incubated for 24h at 37°C/5% CO2. Cells were then transfected with or without 500 ng/well pcDNA3.1 plasmid

encoding SNAP/NRP1 or SNAP/β2AR (as a negative control) and incubated for a further 24h before seeding into poly-D-lysine coated white flat bottom 96 well plates at 60,000 cells/well and incubated for 24h at 37°C/5% CO_2. Assays were performed as above in triplicate wells. To determine basal BRET, SNAP-tagAF488 was omitted during labelling. Sequential filtered light emissions were recorded using a PHERAStar FS plate reader using 475 nm (30 nm bandpass) and 535 nm (30 nm bandpass) filters. BRET ratios were calculated by dividing the 535 nm emission (acceptor) by the 475 nm emission (donor).

To assess the effect of fusion of HiBiT to the C-terminus of CXCL17. HEK293 cells were seeded in 6 well plates at 300,000 cells per well and incubated for 24h at 37°C/5% CO_2. Cells were then transfected as per the BRET β-arrestin2 recruitment assay protocol or G protein activation assays as described above and incubated for a further 24h before co-seeded into poly-D-lysine coated white flat bottom 96 well plates at 30,000 cells/well with wildtype HEK293 cells or HEK293 cells stably expressing CXCL17-HiBiT and incubated for 24h at 37°C/5% CO_2. Assays were performed as above as per the β-arrestin2 recruitment BRET assay protocol or G protein activation assays BRET protocol in triplicate wells.

CXCL17 conservation analysis

Conservation analysis was performed by WebLogo[55] using the multiple sequence alignment of forty-five 119 amino acid CXCL17 orthologues obtained from UniProt[56] (table S2).

Data presentation and statistical analysis

Due to differences in plate reader sensitivity and expression differences between cell lines/assays, raw BRET ratios cannot be compared as a measure of BRET efficacy between Figs as optimised plate reader emission gains were used (table S3) to ensure sufficient sensitivity and/or measurements acquired did not saturate the detector. In general, BRET ratios were calculated by dividing the acceptor emission by the donor emission. Calculation of baseline-corrected BRET ratios or luminescence values are described in the methods for each assay configuration. Where results reported are taken from kinetic reads, points or bars are the maximum ligand-induced change in the BRET ratio.

Prism 8 software was used to analyse ligand-binding curves. For NanoBRET receptor-ligand saturation binding assays, total and non-specific saturation binding curves were simultaneously fitted using the following equation:

$$BRET\ Ratio = \frac{Bmax * [B]}{[B] + KD} + ((M * [B]) + C)$$

where Bmax is the maximal response, [B] is the concentration of fluorescent ligand in nM, KD is the equilibrium dissociation constant in nM, M is the slope of the non-specific binding component and C is the intercept with the Y-axis.

Concentration-response data were fitted using the following equation:

$$Response = \frac{Emax * [A]}{EC50 + [A]}$$

Where Emax is the maximum response, EC_{50} is the concentration of agonist required to produce 50% of the maximal response and [A] is the agonist concentration. pEC_{50} calculated from maximal change in BRET.

Competition binding or response data were fitted using the following equation:

$$inhibited\ binding\ response = 100 - \frac{100\ X\ [A]}{[A] + (IC50)}$$

where [A] is the concentration of competing ligand, IC_{50} is the molar concentration of this competing ligand required to inhibit 50% of the specific response or binding.

In binding studies, the Cheng-Prusoff equation was used to correct fitted IC_{50} values to K_i values:

$$Ki = \frac{IC50}{1 + \frac{[L]}{KD}}$$

Where [L] is the concentration of fluorescent ligand in nM and K_D is the dissociation constant of fluorescent ligand in nM. K_D values calculated from saturation binding experiments[27].

Statistical analysis was performed using Prism 7 or 8 software (GraphPad, San Diego, USA) using one or two-way ANOVA with an appropriate multiple comparison's test where required or paired t-test. Specific statistical tests used are indicated in the Fig legends and were performed on the mean data of individual experiments (n) also indicated in the Fig legends. Unless otherwise stated date represent mean data of N-individual experiments. For clarity N-values in the figure legends represent the number of individual experiments performed, with each individual experiment was performed in duplicate or triplicate wells as outlined above in the methods section for each experiment. p-value <0.05 was considered statistically significant.

List of Supplementary Materials

Supplementary Figures

Supplementary Tables

Acknowledgements:

This work was supported by MRC (grant numbers MR/N020081/1 and MR/W016176/1), the European Union (H2020-MSCA program grant agreements 641833-ONCORNET and 860229-ONCORNET 2.0) and the ARC Centre for Personalised Therapeutics Technologies (IC170100016). C.W.W. was supported by an NHMRC CJ Martin Fellowship (1088334) and by a UWA fellowship support grant. L.E.K. is supported by a University of Nottingham Anne McLaren Research Fellowship. N.D. is supported by an Australian Government Research Training Program Scholarship and a University of Western Australia Baillieu Research Scholarship. The authors would like to thank Heng See for technical assistance with preliminary experiments and Dr. Brigit Caspar for generation of CXCR4 expression plasmids and cell lines. Figs 6 f-g were created using BioRender.

Author contributions:

C.W.W conceived the study. C.W.W., K.D.G.P and S.J.H supervised the project. C.W.W., L.E.K., M.J.S, N.K., B.K., and S.D generated reagents. C.W.W., S.P., L.E.K., N.D. and R.A. conducted the experiments. C.W.W, S.P. and L.E.K. performed the data analysis. C.W.W., S.P., L.E.K., K.D.G.P., and S.J.H. wrote or contributed to the writing of the manuscript.

Declaration of competing interests.

K.D.G.P. has received funding from Promega, BMG Labtech and Dimerix as Australian Research Council Linkage Grant participating organisations. These organisations played no role in any aspect of the manuscript. C.W.W. is a current employee of Dimerix. KDGP is Chief Scientific Advisor to Dimerix, of which he maintains a shareholding. The authors declare no other competing interests.

Data and materials availability.

Materials are available by reasonable request to the corresponding authors. All data needed to evaluate the conclusions in the paper are present in the paper or the Supplementary Materials

References

1. Mollica Poeta, V., Massara, M., Capucetti, A. & Bonecchi, R. Chemokines and Chemokine Receptors: New Targets for Cancer Immunotherapy. *Frontiers in Immunology* vol. 10 379 (2019).

2. Scholten, D. J. *et al.* Pharmacological modulation of chemokine receptor function. *Br. J. Pharmacol.* **165**, 1617–1643 (2012).

3. Burkhardt, A. M. *et al.* CXCL17 is a major chemotactic factor for lung macrophages. *J Immunol* **193**, 1468–1474 (2014).

4. Pisabarro, M. T. *et al.* Cutting edge: novel human dendritic cell- and monocyte-attracting chemokine-like protein identified by fold recognition methods. *J Immunol* **176**, 2069–2073 (2006).

5. Burkhardt, A. M. *et al.* CXCL17 is a mucosal chemokine elevated in idiopathic pulmonary fibrosis that exhibits broad antimicrobial activity. *J Immunol* **188**, 6399–6406 (2012).

6. Lee, W. Y., Wang, C. J., Lin, T. Y., Hsiao, C. L. & Luo, C. W. CXCL17, an orphan chemokine, acts as a novel angiogenic and anti-inflammatory factor. *Am J Physiol Endocrinol Metab* **304**, E32-40 (2013).

7. Guo, Y. J., Zhou, Y. J., Yang, X. L., Shao, Z. M. & Ou, Z. L. The role and clinical significance of the CXCL17-CXCR8 (GPR35) axis in breast cancer. *Biochem Biophys Res Commun* **493**, 1159–1167 (2017).

8. Li, L. *et al.* CXCL17 expression predicts poor prognosis and correlates with adverse immune infiltration in hepatocellular carcinoma. *PLoS One* **9**, e110064 (2014).

9. Zhang, K. *et al.* Decreased epithelial and sputum miR-221-3p associates with airway eosinophilic inflammation and CXCL17 expression in asthma. *Am J Physiol Lung Cell Mol Physiol* **315**, L253–L264 (2018).

10. Choreño-Parra, J. A. *et al.* CXCL17 Is a Specific Diagnostic Biomarker for Severe Pandemic Influenza A(H1N1) That Predicts Poor Clinical Outcome. *Front. Immunol.* **12**, 251 (2021).

11. Zhou, Z. *et al.* Heightened Innate Immune Responses in the Respiratory Tract of COVID-19 Patients. *Cell Host Microbe* **27**, 883-890.e2 (2020).

12. Maravillas-Montero, J. L. *et al.* Cutting edge: GPR35/CXCR8 is the receptor of the mucosal

chemokine CXCL17. *J Immunol* **194**, 29–33 (2015).

13. Binti Mohd Amir, N. A. S. *et al.* Evidence for the Existence of a CXCL17 Receptor Distinct from GPR35. *J. Immunol.* **201**, 714–724 (2018).

14. Park, S. J., Lee, S. J., Nam, S. Y. & Im, D. S. GPR35 mediates lodoxamide-induced migration inhibitory response but not CXCL17-induced migration stimulatory response in THP-1 cells; is GPR35 a receptor for CXCL17? *Br J Pharmacol* **175**, 154–161 (2018).

15. Schneditz, G. *et al.* GPR35 promotes glycolysis, proliferation, and oncogenic signaling by engaging with the sodium potassium pump. *Sci Signal* **12**, eaau9048 (2019).

16. Matsui, A. *et al.* CXCL17 expression by tumor cells recruits CD11b+Gr1 high F4/80- cells and promotes tumor progression. *PLoS One* **7**, e44080 (2012).

17. Busillo, J. M. & Benovic, J. L. Regulation of CXCR4 signaling. *Biochim Biophys Acta* **1768**, 952–963 (2007).

18. Walenkamp, A. M. E., Lapa, C., Herrmann, K. & Wester, H.-J. CXCR4 Ligands: The Next Big Hit? *J. Nucl. Med.* **58**, 77S LP-82S (2017).

19. Proudfoot, A. E. I., Johnson, Z., Bonvin, P. & Handel, T. M. Glycosaminoglycan Interactions with Chemokines Add Complexity to a Complex System. *Pharmaceuticals* **10**, 70 (2017).

20. Tanegashima, K. *et al.* CXCL14 is a natural inhibitor of the CXCL12-CXCR4 signaling axis. *FEBS Lett* **587**, 1731–1735 (2013).

21. Pan, W. L. *et al.* Overexpression of CXCR4 synergizes with LL-37 in the metastasis of breast cancer cells. *Biochim. Biophys. Acta - Mol. Basis Dis.* **1864**, 3837–3846 (2018).

22. Zirafi, O. *et al.* Discovery and characterization of an endogenous CXCR4 antagonist. *Cell Rep* **11**, 737–747 (2015).

23. Ward, R. J. *et al.* Chemokine receptor CXCR4 oligomerization is disrupted selectively by the antagonist ligand IT1t. *J. Biol. Chem.* **296**, 100139 (2021).

24. Işbilir, A. *et al.* Advanced fluorescence microscopy reveals disruption of dynamic CXCR4 dimerization by subpocket-specific inverse agonists. *Proc. Natl. Acad. Sci. U. S. A.* **117**, 29144–29154 (2020).

25. Wu, B. *et al.* Structures of the CXCR4 chemokine receptor in complex with small molecule

and cyclic peptide antagonists. *Science (80-.).* **330**, 1066–1071 (2010).

26. White, C. W., Kilpatrick, L. E., Pfleger, K. D. G. & Hill, S. J. A nanoluciferase biosensor to investigate endogenous chemokine secretion and receptor binding. *iScience* **24**, 102011 (2021).

27. White, C. W., Caspar, B., Vanyai, H. K., Pfleger, K. D. G. G. & Hill, S. J. CRISPR-Mediated Protein Tagging with Nanoluciferase to Investigate Native Chemokine Receptor Function and Conformational Changes. *Cell Chem. Biol.* **27**, 499-510.e7 (2020).

28. Le Gonidec, S. *et al.* Protamine is an antagonist of apelin receptor, and its activity is reversed by heparin. *Faseb j* **31**, 2507–2519 (2017).

29. Dyer, D. P., Salanga, C. L., Volkman, B. F., Kawamura, T. & Handel, T. M. The dependence of chemokine-glycosaminoglycan interactions on chemokine oligomerization. *Glycobiology* **26**, 312–326 (2016).

30. Graham, G. J., Handel, T. M. & Proudfoot, A. E. I. Leukocyte Adhesion: Reconceptualizing Chemokine Presentation by Glycosaminoglycans. *Trends Immunol.* **40**, 472–481 (2019).

31. Lemmon, M. A. & Schlessinger, J. Cell signaling by receptor tyrosine kinases. *Cell* vol. 141 1117–1134 (2010).

32. Peach, C. J. *et al.* Molecular pharmacology of VEGF-A isoforms: Binding and signalling at VEGFR2. *International Journal of Molecular Sciences* vol. 19 1264 (2018).

33. Peach, C. J. *et al.* Real-Time Ligand Binding of Fluorescent VEGF-A Isoforms that Discriminate between VEGFR2 and NRP1 in Living Cells. *Cell Chem. Biol.* **25**, 1208-1218.e5 (2018).

34. Kilpatrick, L. E. *et al.* Real-time analysis of the binding of fluorescent VEGF165a to VEGFR2 in living cells: Effect of receptor tyrosine kinase inhibitors and fate of internalized agonist-receptor complexes. *Biochem Pharmacol* **136**, 62–75 (2017).

35. Weinstein, E. J. *et al.* VCC-1, a novel chemokine, promotes tumor growth. *Biochem Biophys Res Commun* **350**, 74–81 (2006).

36. Choreño-Parra, J. A., Thirunavukkarasu, S., Zúñiga, J. & Khader, S. A. The protective and pathogenic roles of CXCL17 in human health and disease: Potential in respiratory medicine. *Cytokine and Growth Factor Reviews* vol. 53 53–62 (2020).

37. Travaglini, K. J. *et al.* A molecular cell atlas of the human lung from single-cell RNA sequencing. *Nature* **587**, 619–625 (2020).

38. Zhang, W. *et al.* A Point Mutation That Confers Constitutive Activity to CXCR4 Reveals That T140 Is an Inverse Agonist and That AMD3100 and ALX40-4C Are Weak Partial Agonists. *J. Biol. Chem.* **277**, 24515–24521 (2002).

39. Mona, C. E. *et al.* Design, synthesis, and biological evaluation of CXCR4 ligands. *Org. Biomol. Chem.* **14**, 10298–10311 (2016).

40. Winer, M. A. & Ax, R. L. Properties of heparin binding to purified plasma membranes from bovine granulosa cells. *J. Reprod. Fertil.* **87**, 337–348 (1989).

41. Crijns, H., Vanheule, V. & Proost, P. Targeting Chemokine—Glycosaminoglycan Interactions to Inhibit Inflammation . *Frontiers in Immunology* vol. 11 483 (2020).

42. Shintani, Y. *et al.* Glycosaminoglycan modification of neuropilin-1 modulates VEGFR2 signaling. *EMBO J* **25**, 3045–3055 (2006).

43. Verkaar, F. *et al.* Chemokine cooperativity is caused by competitive glycosaminoglycan binding. *J Immunol* **192**, 3908–3914 (2014).

44. Hamon, M. *et al.* A syndecan-4/CXCR4 complex expressed on human primary lymphocytes and macrophages and HeLa cell line binds the CXC chemokine stromal cell-derived factor-1 (SDF-1). *Glycobiology* **14**, 311–323 (2004).

45. Charnaux, N. *et al.* Syndecan-4 is a signaling molecule for stromal cell-derived factor-1 (SDF-1)/ CXCL12. *Febs j* **272**, 1937–1951 (2005).

46. Xiao, H. *et al.* Selective CXCR4 antagonism by Tat: Implications for in vivo expansion of coreceptor use by HIV-1. *Proc. Natl. Acad. Sci. U. S. A.* **97**, 11466–11471 (2000).

47. Alexander, S. P. *et al.* THE CONCISE GUIDE TO PHARMACOLOGY 2017/18: G protein-coupled receptors. *Br J Pharmacol* **174 Suppl**, S17-s129 (2017).

48. Ibrahimi, O. A., Zhang, F., Hrstka, S. C. L., Mohammadi, M. & Linhardt, R. J. Kinetic Model for FGF, FGFR, and Proteoglycan Signal Transduction Complex Assembly. *Biochemistry* **43**, 4724–4730 (2004).

49. Kilpatrick, L. E. E. *et al.* Complex Formation between VEGFR2 and the β<inf>2</inf>-Adrenoceptor. *Cell Chem Biol* **26**, 830-841 e9 (2019).

50. See, H. B., Seeber, R. M., Kocan, M., Eidne, K. A. & Pfleger, K. D. Application of G protein-coupled receptor-heteromer identification technology to monitor beta-arrestin recruitment to G protein-coupled receptor heteromers. *Assay Drug Dev Technol* **9**, 21–30 (2011).

51. White, C. W., Vanyai, H. K., See, H. B., Johnstone, E. K. M. & Pfleger, K. D. G. Using nanoBRET and CRISPR/Cas9 to monitor proximity to a genome-edited protein in real-time. *Sci. Rep.* **7**, 1–14 (2017).

52. Kocan, M. *et al.* Agonist-independent interactions between beta-arrestins and mutant vasopressin type II receptors associated with nephrogenic syndrome of inappropriate antidiuresis. *Mol Endocrinol* **23**, 559–571 (2009).

53. Ayoub, M. A. *et al.* Functional interaction between angiotensin II receptor type 1 and chemokine (C-C motif) receptor 2 with implications for chronic kidney disease. *PLoS One* **10**, e0119803 (2015).

54. Bouzo-Lorenzo, M. *et al.* A live cell NanoBRET binding assay allows the study of ligand-binding kinetics to the adenosine A3 receptor. *Purinergic Signal* **15**, 139–153 (2019).

55. Crooks, G. E., Hon, G., Chandonia, J.-M. & Brenner, S. E. WebLogo: A Sequence Logo Generator. *Genome Res.* **14**, 1188–1190 (2004).

56. Consortium, T. U. UniProt: a worldwide hub of protein knowledge. *Nucleic Acids Res.* **47**, D506–D515 (2018).

Figure Legends

Fig 1: CXCL17 inhibits constitutive, and ligand-induced CXCR4 signalling. (A) HEK293 cells transiently transfected with CCR1-10 or CXCR1-3,5 or 6, $G\alpha_{i1}$/Nluc and Venus/$G\gamma_2$ were stimulated with CXCL17, submaximal concentrations of chemokines, CXCL17, or their corresponding chemokine ligands, and their BRET ratios measured. **(B)** Kinetic analysis of changes in BRET following application of CXCL12, CXCL17 or both CXCL12 and CXCL17 in HEK293 cells transiently-transfected with CXCR4, $G\alpha_{i1}$/Nluc and Venus/$G\gamma_2$. **(C)** BRET in HEK293 cells transiently transfected with CXCR4, $G\alpha_{i1}$/Nluc and Venus/$G\gamma_2$ and treated with CXCL12 by increasing concentrations of AMD3100 or CXCL17. **(D)** HEK293G cells stably-expressing the cAMP GloSensor transgene and SNAP/CXCR4 were stimulated with buffer, forskolin, or forskolin and CXCL12, in the absence or presence of CXCL17 or AMD3100 . For **B,** ligand was added following establishment of basal BRET and is indicated on the x-axis as ligand. Points or bars represent mean ± s.e.m. of N=4 (**A**), N=4 (**B**), N=4 (**C**) and N=4 (**D**) individual experiments. **(D)** bars represent mean % ± s.e.m. of the forskolin-mediated response of each individual experiment. n.s., non-significant*, $p<0.05$ and **, $p<0.01$, indicates a significant difference between the paired groups or group and baseline. Statistical analysis by one-way **(D)** or two-way (**A and B**) ANOVA with a Dunnett's multiple comparisons test.

Fig 2: CXCL17 inhibits constitutive, and ligand-induced CXCR4-β-arrestin2 interactions. (A) HEK293 cells transiently-transfected with CXCR4/Rluc8 and β-arrestin2/Venus were stimulated at time *ligand t1* with HBSS or CXCL12 then at time *ligand t2* stimulated again with HBSS or CXCL17. **(B**) Change in BRET following application of increasing concentrations of CXCL17 to HEK293 cells transiently-transfected with CXCR4/Rluc8 and β-arrestin2/Venus. **(C)** HEK293 cells transiently-transfected with CXCR4/NLuc and β-arrestin2/Venus were stimulated with CXCL12 in the absence or presence of AMD3100 or CXCL17. **(D)** HEK293 cells transiently-transfected with CXCR1/Rluc8, CCR5/Rluc8 or β_2-adrenoceptor/Rluc8 and β-arrestin2/Venus were stimulated with CXCL17, CXCL8, CCL5 or isoprenaline respectively. Points or bars represent mean ± s.e.m. of , N=3 **(A)**, N=3, **(B)**, N=3 **(D)** or N=6, **(C)**. **$p<0.01$, ***, $p<0.01$, and ****, $p<0.0001$ indicates a significant difference between the paired groups or baseline. Statistical analysis by one-way **(D)** or two-way (**A**) ANOVA with a Dunnett's multiple comparisons test.

Fig 3: CXCL17 binding to CXCR4 is context dependent. Live **(A)** HEK293 cells or **(B)** membrane preparations stably-expressing NLuc/CXCR4 were incubated with CXCL12-AF647 and increasing concentrations of AMD3100 or CXCL17. **(C)** Confocal imaging of HEK293 cells stably-expressing

SNAP/CXCR4 under unstimulated conditions or after treatment with CXCL12 or CXCL17. Data in (**C)** are representative of N=3 individual experiments. Scale bar represents 20 μm. **(D)** Permeabilised membrane preparations stably-expressing NLuc/CXCR4 were incubated with CXCL12-AF647 in the absence or presence of or CXCL17 . White bar (HBSS) is vehicle control. **(E)** Membrane preparations stably expressing NLuc/CXCR4 were co-incubated with wildtype HEK293 cells and incubated with CXCL12-AF647 and increasing concentrations of AMD3100 or CXCL17. **(F)** HEK293 cells or **(G)** membrane preparations stably-expressing NLuc/CXCR4 were incubated with IT1t-BY630/650 and increasing concentrations of IT1t or CXCL17. Points or bars represent mean ± s.e.m. of N=4, **(A),** N=4, **(B)**, N=4 **(D)**, N=4 **(E)**, N=4, **(F)** or N=5 **(G)** individual experiments. ****, $p<0.0001$ indicates a significant difference between the paired groups or baseline. Statistical analysis by one-way ANOVA with a Dunnett's multiple comparisons test. For panels **B,E,F and G** a t-test was performed between the highest concentration of CXCL17 used and fluorescent ligand only, no significant differences were observed $p>0.05$.

Fig 4: Displacement of the binding of secreted genome-edited CXCL12-HiBiT to SNAP/CXCR4 by CXCL17. HEK293 cells expressing genome-edited CXCL12-HiBiT, were transiently transfected with SNAP/CXCR4 and incubated in the absence or presence of increasing concentrations of AMD3100,CXCL17 or Surfen. Bars represent basal BRET in the absence of added AlexaFluor488 label. Bars and points represent mean ± s.e.m. of N=6 individual experiments

Fig 5: Binders of glycosaminoglycans mimic the effect of CXCL17. (A) Sequence of human CXCL17 with putative GAG binding domains highlighted in red. **(B-E) effect of GAG binders on ligand binding to Nluc/CXCR4.** Live HEK293 cells **(B and C)** or membrane preparations **(D and E)** expressing Nluc/CXCR4, were incubated with CXCL12-AF647 (**B_E**) and increasing concentrations of surfen **B and D**) or protamine sulfate (**C and E**), CXCL12 (**B and D**) or AMD3100 (**C and E**). Points represent mean ± s.e.m. of N=4,**B)**, N=5, **(C),** N=4 **(D**), and N=5 **(E)** individual experiments.

Fig 6: CXCL17 secretion, membrane interaction, and CXCR4 binding is inhibited by disruption of putative GAG domains. (A) Sequence of HiBiT tagged wild type CXCL17 or CXCL17 with the putative GAG domains disrupted through alanine substitution. **(B)** HEK293 cells transfected with CXCL17-HiBiT were treated with CXCL17,surfen or protamine sulfate (PS) with or without heparin sulfate (HS) and luminescence measured. **(C)** Endpoint luminescence reads of **B** and figs S9A and S9D, summarising the change in luminescence induced by different treatments in cells transfected with either wildtype CXCL17-HiBiT or gag -ve CXCL17-HiBiT. **(D)**. HEK293 cells were transfected with wildtype CXCL17- or gag -ve CXCL17-HiBiT and SNAP/CXCR4 with BRET measured in the presence and absence of surfen, protamine sulfate , or AMD3100 . **(E)** Raw luminescence output from HEK293 cells transfected with either CXCL17-HiBiT (black bars) or gag -ve CXCL17-HiBiT. Points or bars represent mean ± s.e.m. of N=5 **(B)**, N=5, **(C)**, N=5, **(D)**, N=5, **(E)** individual experiments. **(C-D)** *, $p<0.05$, ****, $p<0.0001$ calculated by a two-way ANOVA with a Tukey's multiple comparisons test. **(E)** ****, $p<0.0001$ calculated by a Welch's

unpaired t-test **(F-G) Proposed mechanisms of CXCL17-mediated inhibition of CXCR4. (F)** Inhibition of CXCR4 by CXCL17 'bridge' formation between a closely colocalised GAG-containing proteoglycan and CXCR4. **(G)** CXCL17-promoted clustering of GAG containing proteoglycans around CXCR4 prevents binding of CXCL12 but allows binding of small molecule inhibitors.

Fig 7: CXCL17 interacts with NRP1 but not VEGFR2. NanoBRET competition ligand binding in live HEK293 cells expressing **(A)** NLuc/VEGFR2 or **(B)** NLuc/NRP1. Cells were incubated with $VEGF_{165}$a-TMR in the absence of other ligands or in the presence of, CXCL17,CXCL12 or $VEGF_{165}$a. Black bar (HBSS) represents vehicle control. **(C)** HEK293 cells expressing CXCL17-HiBiT were transfected with SNAP/NRP1 and incubated in the absence or presence of surfen or protamine sulfate. Bars represent mean ± s.e.m. of N=4 **(A)**, N=4, **(B)** or N=5 **(C)** individual. Data is non-significant unless otherwise specified. n.s., non-significant, *, $p<0.05$, **, $p<0.01$, ***, $p>0.001$, ****, $p<0.0001$ calculated by one-way ANOVA with Dunnett's multiple comparisons test.

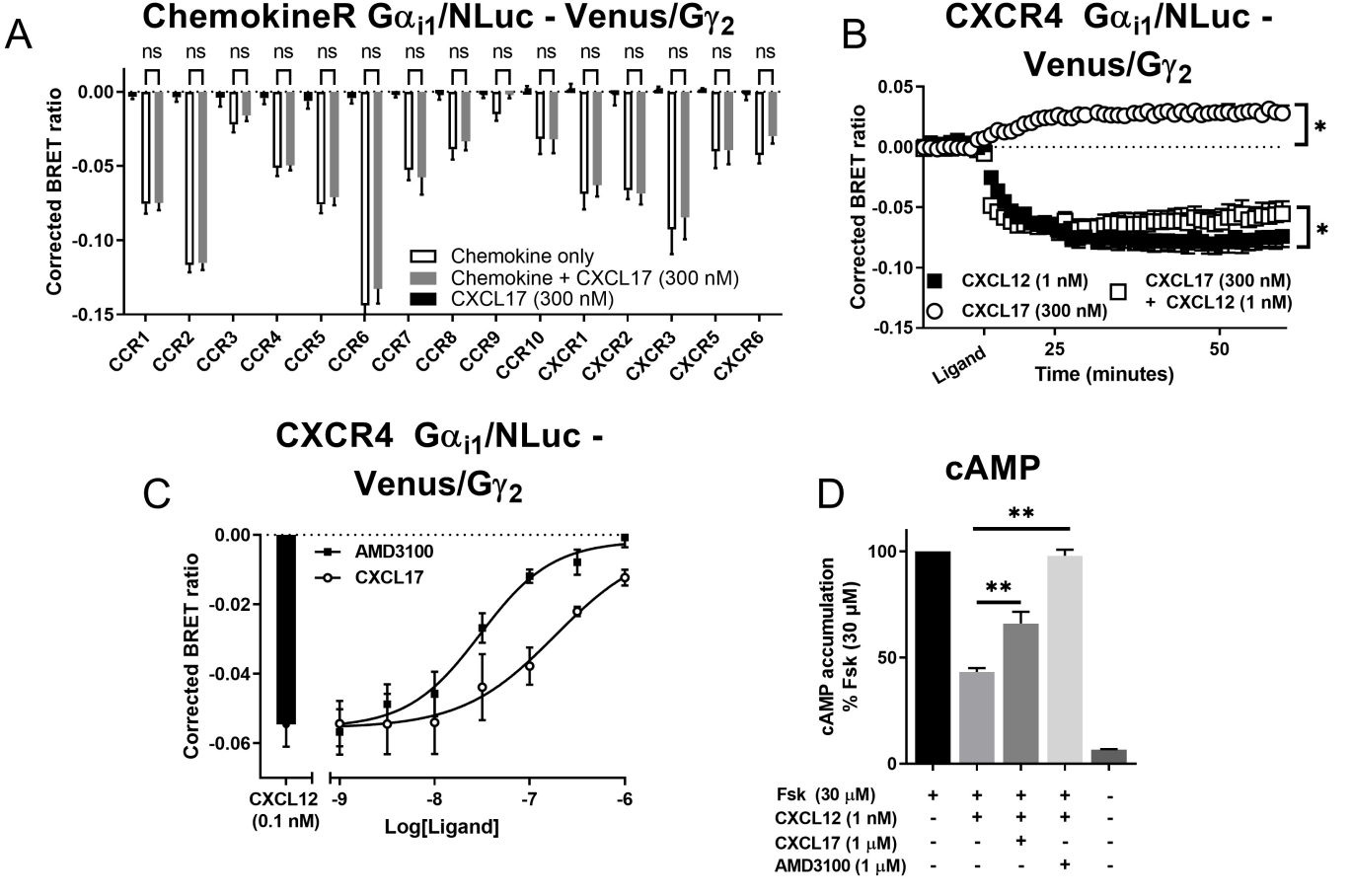
A
ChemokineR Gαi1/NLuc - Venus/Gγ2
ns
Corrected BRET ratio
0.00
-0.05
-0.10
-0.15
Chemokine only
Chemokine + CXCL17 (300 nM)
CXCL17 (300 nM)
CCR1
CCR2
CCR3
CCR4
CCR5
CCR6
CCR7
CCR8
CCR9
CCR10
CXCR1
CXCR2
CXCR3
CXCR5
CXCR6
B
CXCR4 Gαi1/NLuc - Venus/Gγ2
0.05
CXCL12 (1 nM)
CXCL17 (300 nM)
CXCL17 (300 nM) + CXCL12 (1 nM)
*
Ligand
25
50
Time (minutes)
C
CXCR4 Gαi1/NLuc - Venus/Gγ2
AMD3100
CXCL17
CXCL12 (0.1 nM)
-9
-8
-7
-6
Log[Ligand]
D
cAMP
cAMP accumulation % Fsk (30 μM)
100
50
0
**
Fsk (30 μM)
CXCL12 (1 nM)
CXCL17 (1 μM)
AMD3100 (1 μM)

CXCR4 - β-arrestin2 recruitment

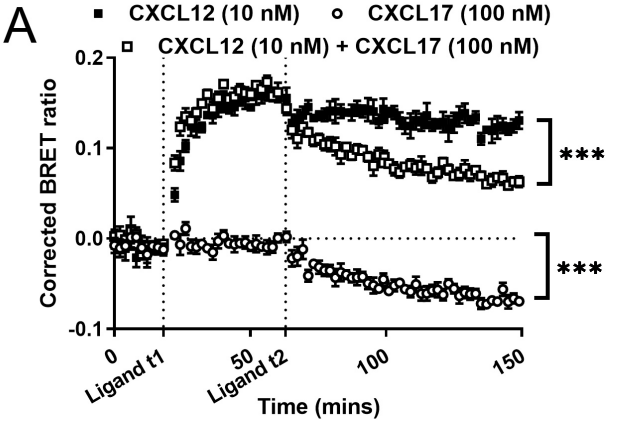

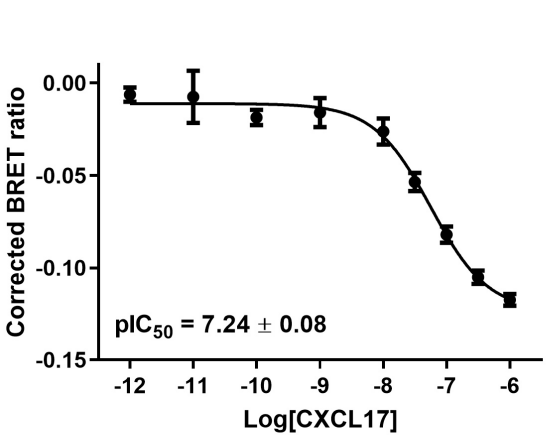

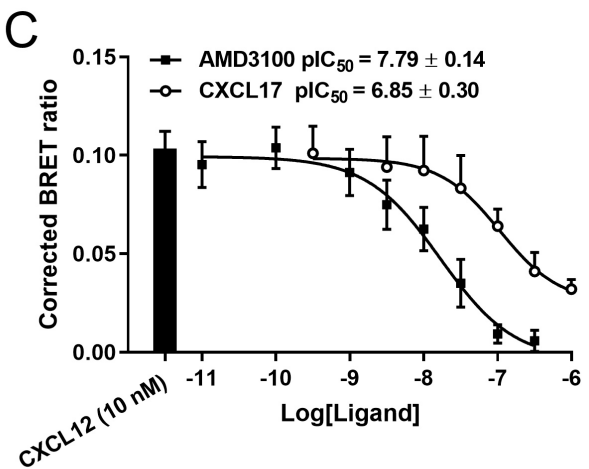

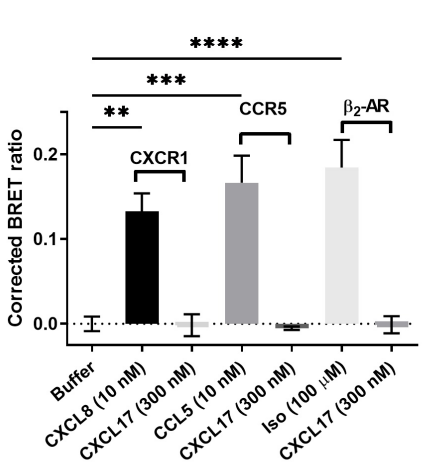

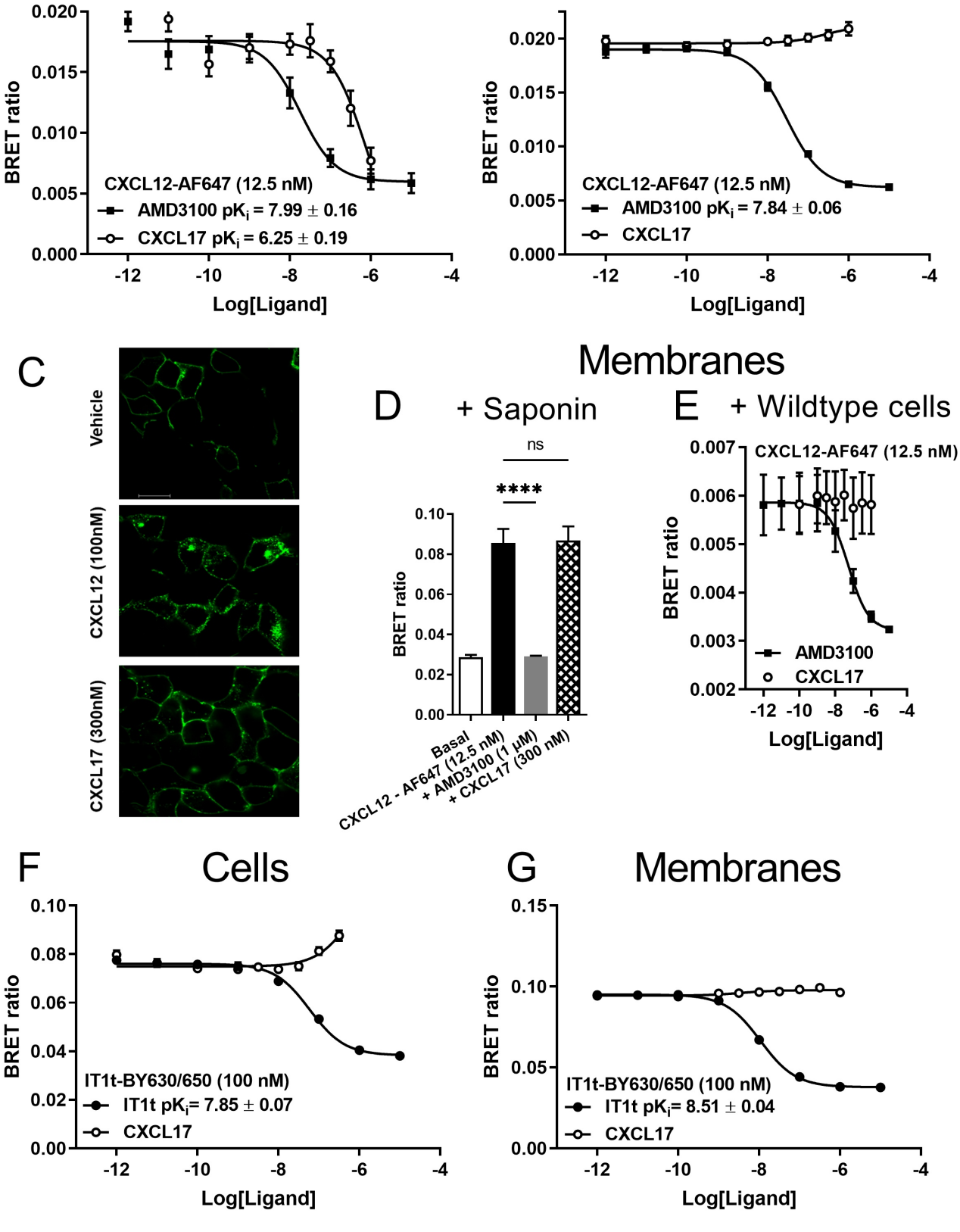
A
Cells
BRET ratio
0.020
0.015
0.010
0.005
0.000
-12
-10
-8
-6
-4
Log[Ligand]
CXCL12-AF647 (12.5 nM)
AMD3100 pKi = 7.99 ± 0.16
CXCL17 pKi = 6.25 ± 0.19
B
Membranes
BRET ratio
Log[Ligand]
CXCL12-AF647 (12.5 nM)
AMD3100 pKi = 7.84 ± 0.06
CXCL17
C
Membranes
Vehicle
CXCL12 (100nM)
CXCL17 (300nM)
D
+ Saponin
ns
****
BRET ratio
0.10
0.08
0.06
0.04
0.02
0.00
Basal
CXCL12 - AF647 (12.5 nM)
+ AMD3100 (1 µM)
+ CXCL17 (300 nM)
E
+ Wildtype cells
CXCL12-AF647 (12.5 nM)
BRET ratio
0.007
0.006
0.005
0.004
0.003
0.002
AMD3100
CXCL17
-12
-10
-8
-6
-4
Log[Ligand]
F
Cells
BRET ratio
0.10
0.08
0.06
0.04
0.02
0.00
IT1t-BY630/650 (100 nM)
IT1t pKi= 7.85 ± 0.07
CXCL17
-12
-10
-8
-6
-4
Log[Ligand]
G
Membranes
BRET ratio
0.15
0.10
0.05
0.00
IT1t-BY630/650 (100 nM)
IT1t pKi= 8.51 ± 0.04
CXCL17
-12
-10
-8
-6
-4
Log[Ligand]

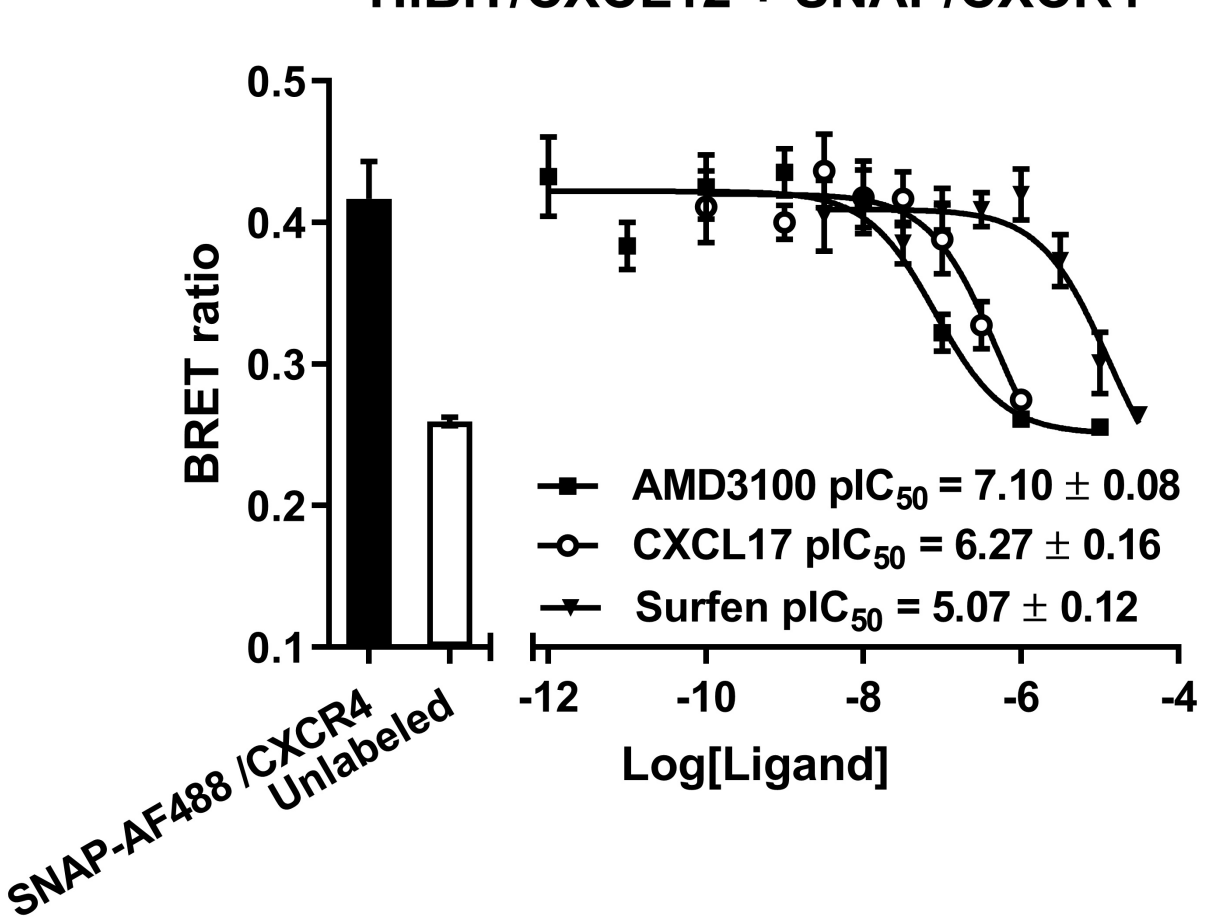
HiBiT/CXCL12 + SNAP/CXCR4
BRET ratio
0.5
0.4
0.3
0.2
0.1
SNAP-AF488 /CXCR4
Unlabeled
AMD3100 pIC50 = 7.10 ± 0.08
CXCL17 pIC50 = 6.27 ± 0.16
Surfen pIC50 = 5.07 ± 0.12
-12
-10
-8
-6
-4
Log[Ligand]

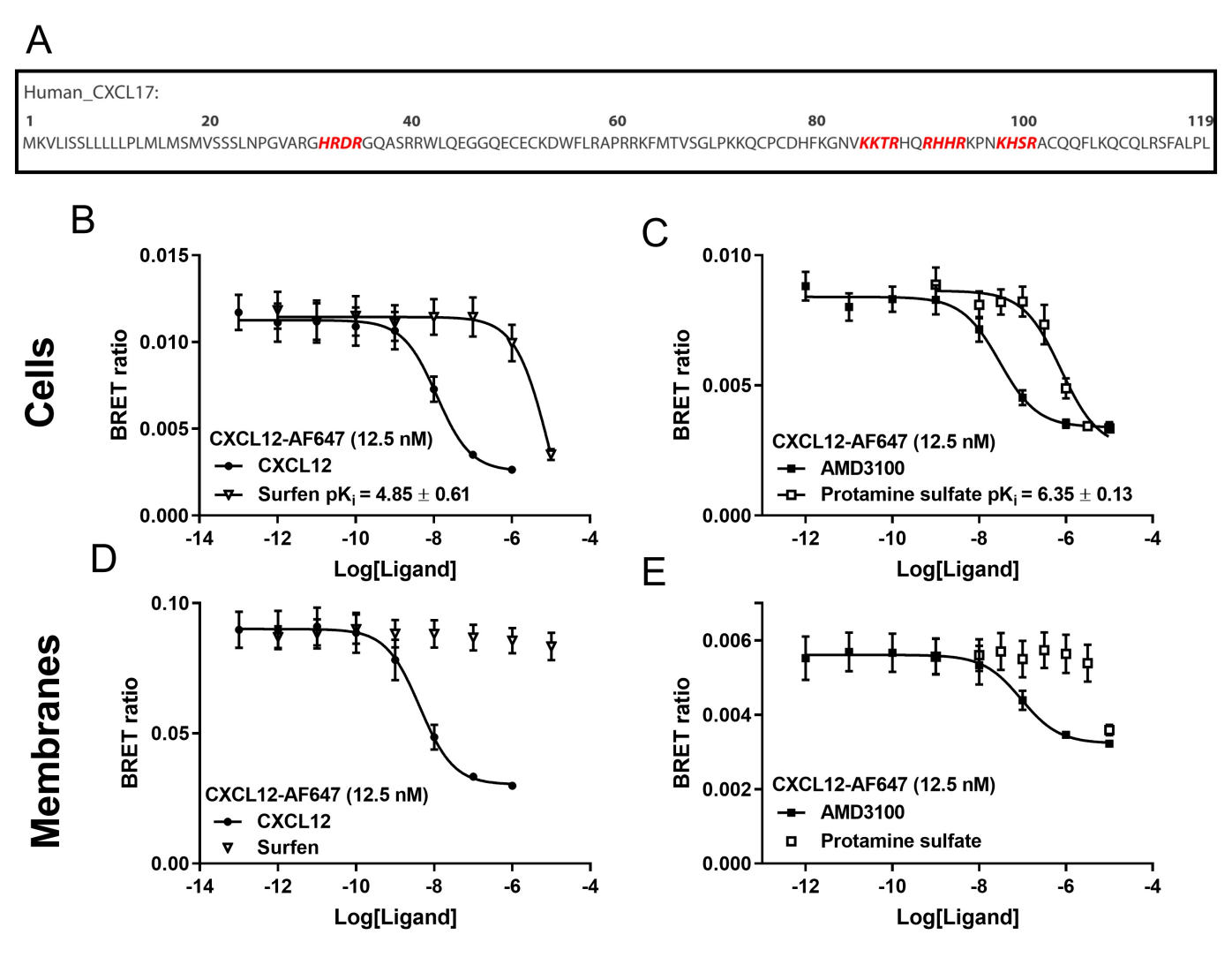
A
Human_CXCL17:
1 20 40 60 80 100 119
MKVLISSLLLLLPLMLMSMVSSSLNPGVARGHRDRGQASRRWLQEGGQECECKDWFLRAPRRKFMTVSGLPKKQCPCDHFKGNVKKTRHQRHHRKPNKHSRACQQFLKQCQLRSFALPL
B
C
D
E
Cells
Membranes
BRET ratio
Log[Ligand]
CXCL12-AF647 (12.5 nM)
CXCL12
Surfen pKi = 4.85 ± 0.61
AMD3100
Protamine sulfate pKi = 6.35 ± 0.13
Surfen
Protamine sulfate

A

```
WT CXCL17HiBiT     MKVLISSLLLLLPLMLMSMVSSSLNPGVARGHRDRGQASRRWLQEGGQECECKDWFLRAPRRKFMTVSGLPKKQCPCDHFKGNVKKTRHQRHHRKPNKHSRACQQFLKQCQLRSFALPLGSSGVSGWRLFKKIS*
Mutant CXCL17HiBiT .............................AA.A.....................................................AA.A..AA.A...AA.A.....................................*
Signal Peptide. CXCL17. Linker. HiBiT.
```

B

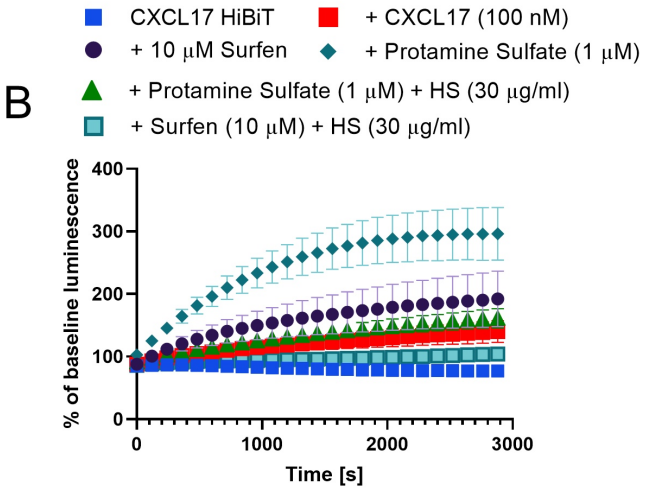

C

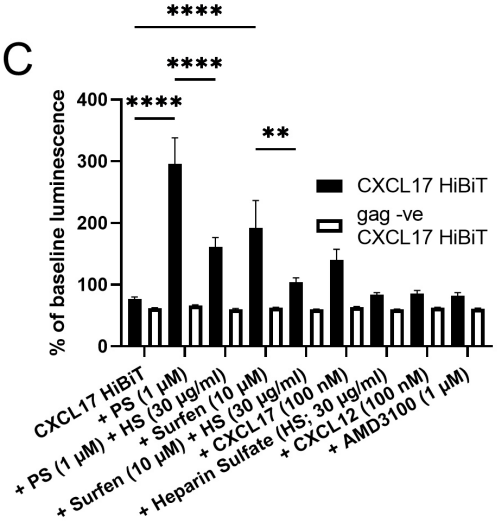

CXCL17-HiBiT + SNAP/CXCR4

D

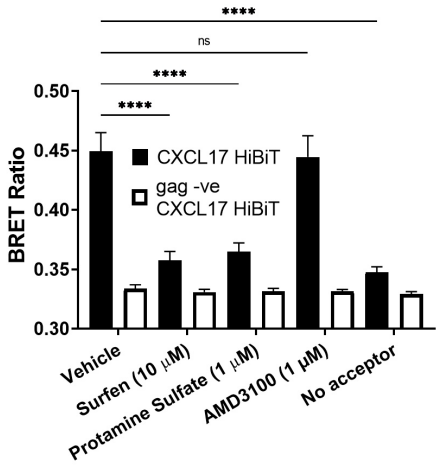

E

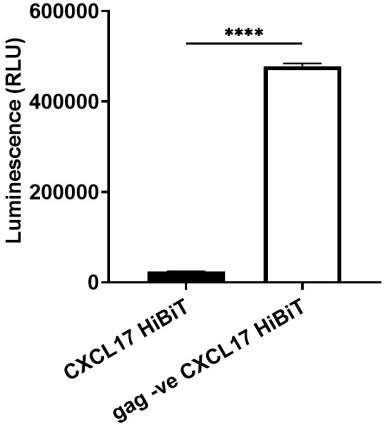

F

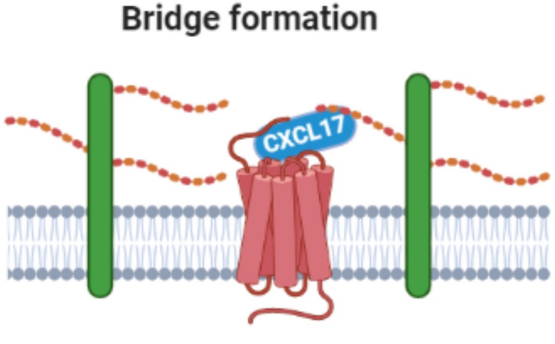

G

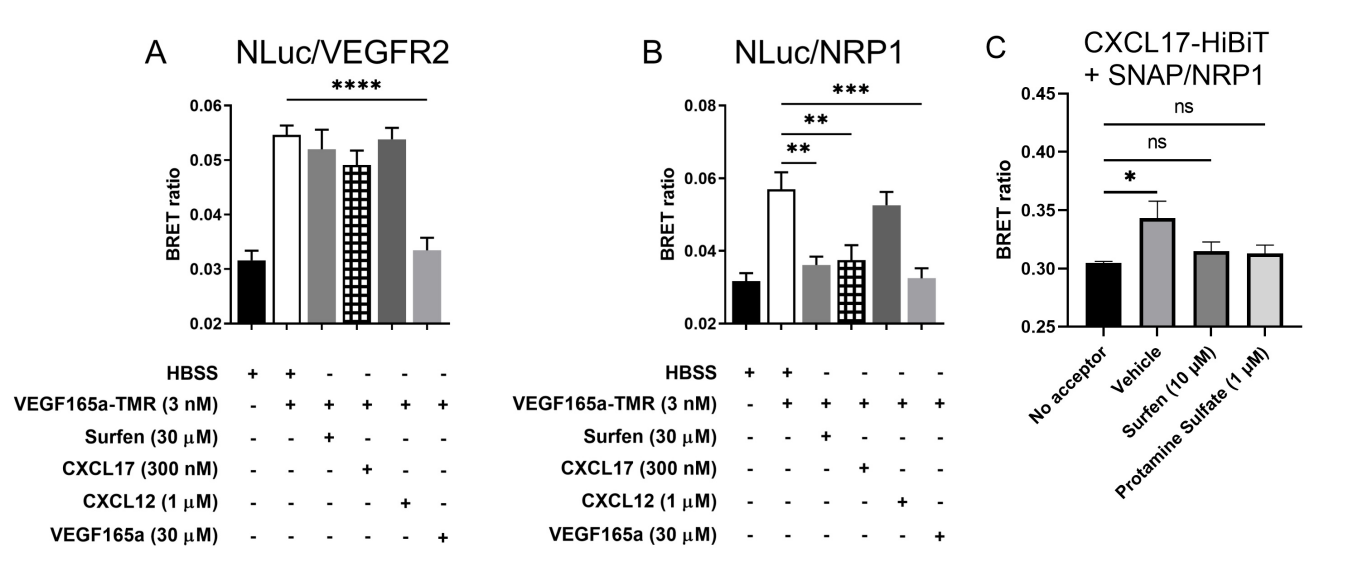
A
NLuc/VEGFR2
****
BRET ratio
0.06
0.05
0.04
0.03
0.02
HBSS + + - - - -
VEGF165a-TMR (3 nM) - + + + + +
Surfen (30 μM) - - + - - -
CXCL17 (300 nM) - - - + - -
CXCL12 (1 μM) - - - - + -
VEGF165a (30 μM) - - - - - +
B
NLuc/NRP1
***
**
**
BRET ratio
0.08
0.06
0.04
0.02
HBSS + + - - - -
VEGF165a-TMR (3 nM) - + + + + +
Surfen (30 μM) - - + - - -
CXCL17 (300 nM) - - - + - -
CXCL12 (1 μM) - - - - + -
VEGF165a (30 μM) - - - - - +
C
CXCL17-HiBiT
+ SNAP/NRP1
ns
ns
*
BRET ratio
0.45
0.40
0.35
0.30
0.25
No acceptor
Vehicle
Surfen (10 μM)
Protamine Sulfate (1 μM)

Supplementary Materials

Fig S1

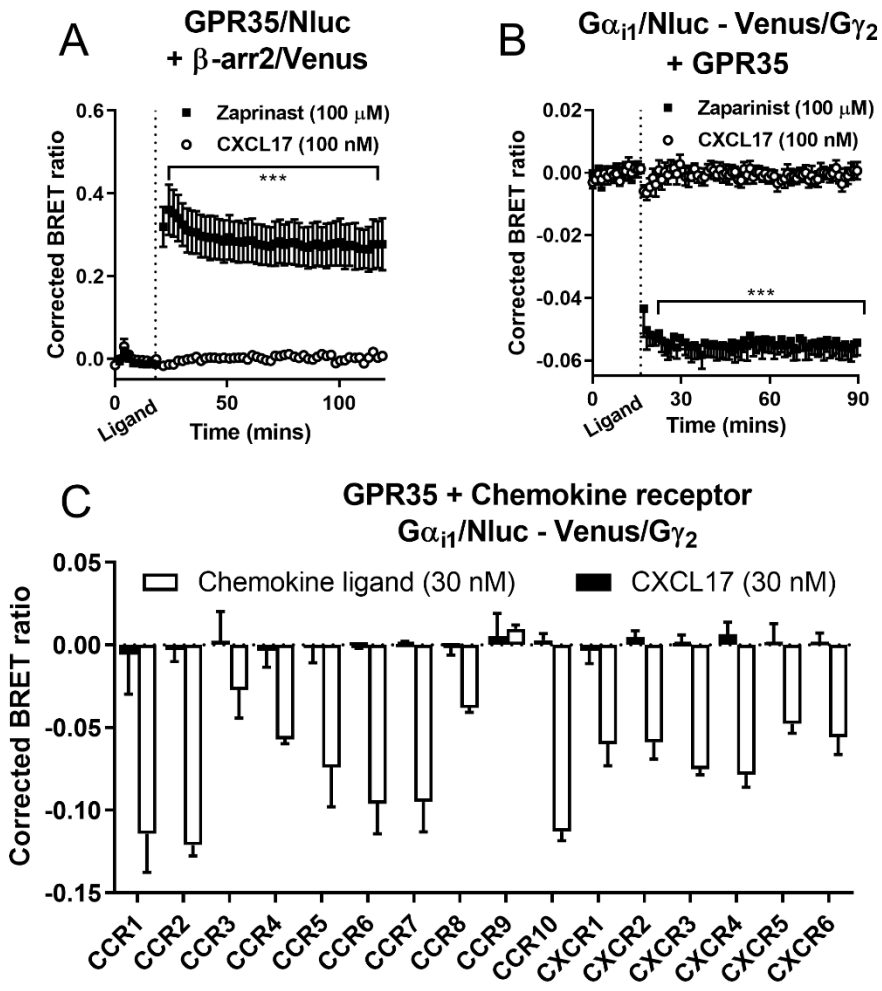

Fig S1: CXCL17 does not activate GPR35. (A) HEK293 cells transiently transfected with GPR35/NLuc and β-arrestin2/Venus were stimulated with zaprinast or CXCL17. **(B)** HEK293 cells transiently transfected with GPR35, $G\alpha_{i1}$/NLuc and Venus/$G\gamma_2$ were stimulated with zaprinast or CXCL17 . **(C)** Maximum change in BRET observed in HEK293 cells transiently-transfected with GPR35, $G\alpha_{i1}$/NLuc and Venus/$G\gamma_2$ plus CCR1-CCR10 or CXCR1-6 following application of the endogenous chemokine ligand or CXCL17. Points or bars represent mean ± s.e.m. of N=3 individual experiments **(A-B)** or mean ± range of N=2 individual experiments (**C**). **, $p<0.001$ by two-ANOVA with a Tukey's multiple comparisons test. CXCL17 data points in **(C)** were non-significant compared to baseline.

Fig S2

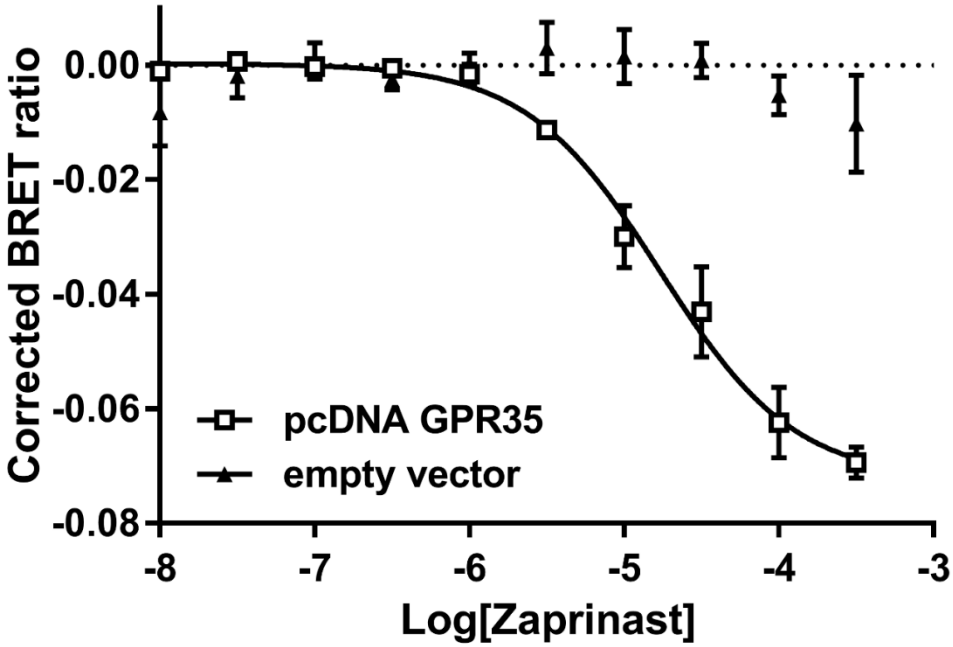

Fig S2: The $G_{\alpha i1}$/NLuc and Venus/$G_{\gamma 2}$ BRET assay measures GPR35 activation. HEK293 cells transiently transfected with $G_{\alpha i1}$/NLuc and Venus/$G_{\gamma 2}$ along with plasmids encoding GPR35 pEC_{50} = 4.76 ± 0.82) or empty vector were stimulated with increasing concentrations of zaprinast. Corrected BRET was calculated as described in Methods. Points represent mean ± s.e.m. of N=3 individual experiments.

Fig S3

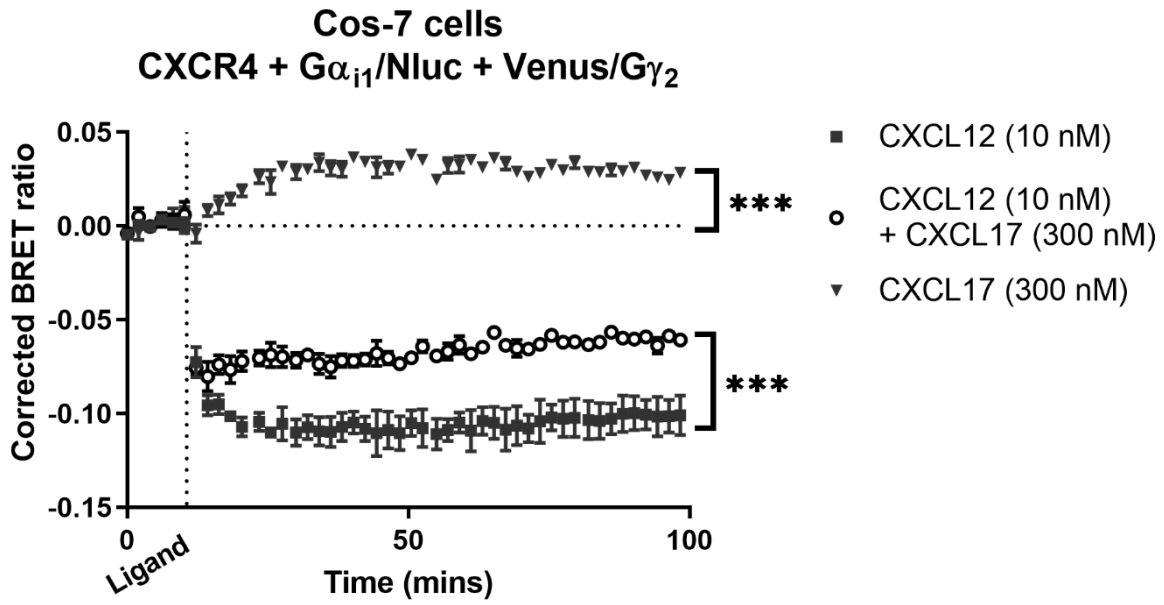

Fig S3: CXCL17 inhibits CXCR4-mediated G protein activation in Cos-7 cells. Cos-7 cells transiently-transfected with Gαi1/NLuc, Venus/$G\gamma_2$ and CXCR4 were stimulated with, CXCL12 and CXCL17 or CXCL17. Corrected BRET was calculated as described in Methods. Points represent mean ± s.e.m. of N=3 individual experiments***, $p<0.01$ versus baseline or CXCL12 only by two-ANOVA with Tukey multiple comparisons test.

Fig S4

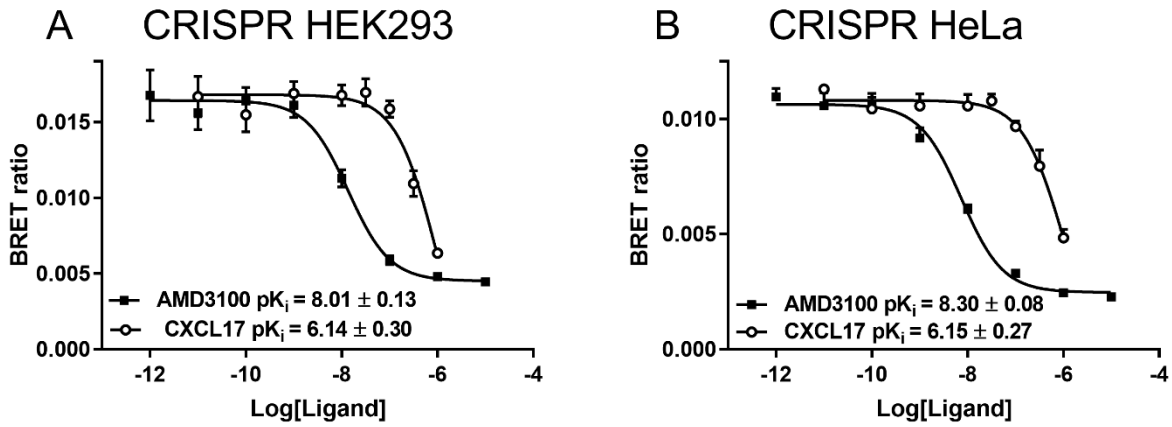

Fig S4: NanoBRET competition ligand binding at NLuc/CXCR4 expressed under endogenous promotion. Displacement of CXCL12-AF647 binding by AMD3100 or CXCL17 in live **(A)** HEK293 cells or **(B)** HeLa cells genome-edited to express NLuc/CXCR4. Points represent mean ± s.e.m. of N=4, **(A)** and N=4, **(B)** individual experiments.

Fig S5

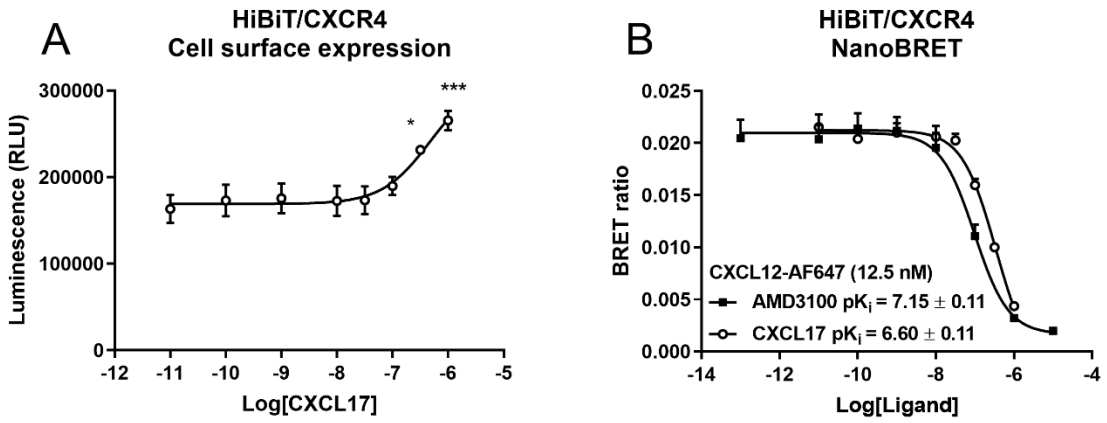

Fig S5: Effect of CXCL17 on CXCR4 cell surface expression and CXCL12-AF647 binding to plasma membrane-localised CXCR4. (A) HEK293 cells stably-expressing HiBiT/CXCR4 were incubated with increasing concentrations of CXCL17 and luminescence measured. **(B)** NanoBRET competition ligand binding curves obtained in HEK293 cells stably-expressing HiBiT/CXCR4 incubated with CXCL12-AF647 and increasing concentrations of CXCL17 or AMD3100. Points represent mean ± s.e.m. of N=4 **(A)** or N=5 **(B)** individual experiments. *, $p<0.05$ and ***, $p<0.001$ by one-way ANOVA with Dunnett's multiple comparisons test.

Fig S6

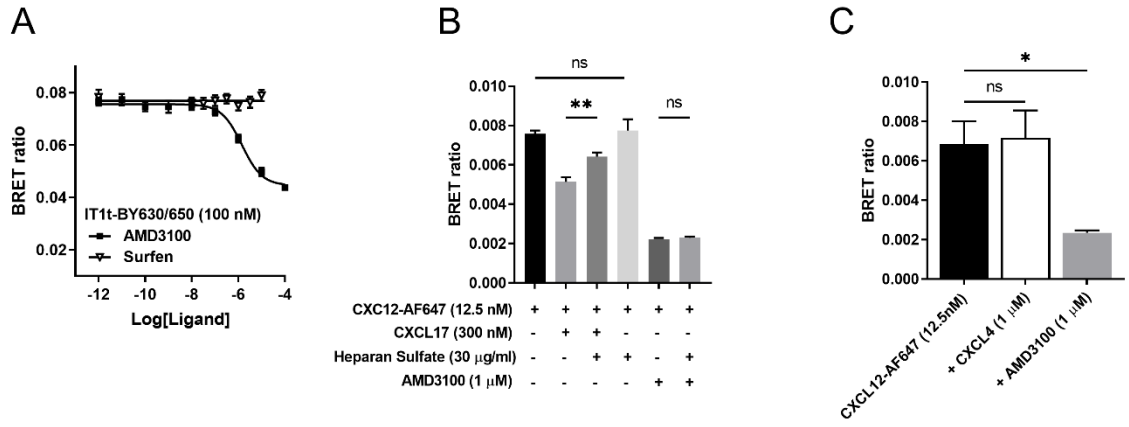

Fig S6: Binders of glycosaminoglycans mimic the effect of CXCL17. (A) Live HEK293 cells expressing NLuc/CXCR4, were incubated with IT1t-BY630/650 and increasing concentrations of surfen or AMD3100. **(B)** Live HEK293 cells expressing genome-edited NLuc/CXCR4 were incubated with CXCL12-AF647 in the absence of other ligands, or in the presence of heparan sulfate , CXCL17 or AMD3100, or in the presence of CXCL17 or AMD3100pre-incubated with heparan sulfate. (**C**) Live HEK293 cells expressing genome-edited NLuc/CXCR4 were incubated with CXCL12-AF647 in the absence of other ligands , or in the presence of AMD3100 or CXCL4 . Points or bars represent mean ± s.e.m. of N=4 (**C**), N=5 **(A)** or N=6 (**B**) individual experiments. *, $p<0.05$ and **, $p<0.01$ and ns, not statistically significant calculated by one-way ANOVA with Tukey's multiple comparisons test. For panel **A** a t-test was performed between the highest concentration of Surfen used and fluorescent ligand only, no significant differences were observed $p>0.05$.

Fig S7:

A

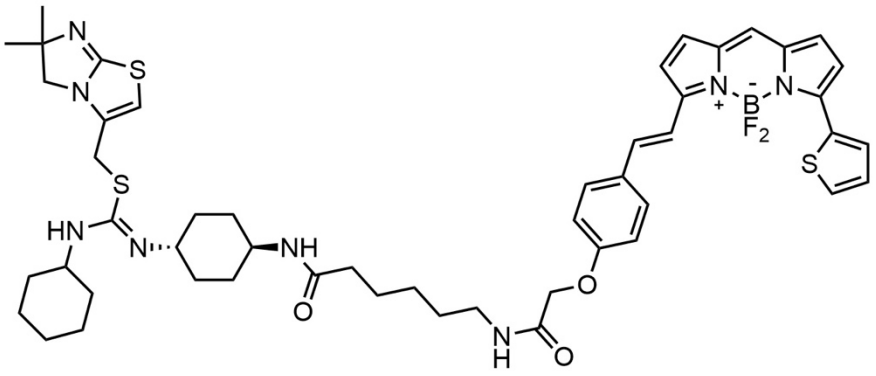

B

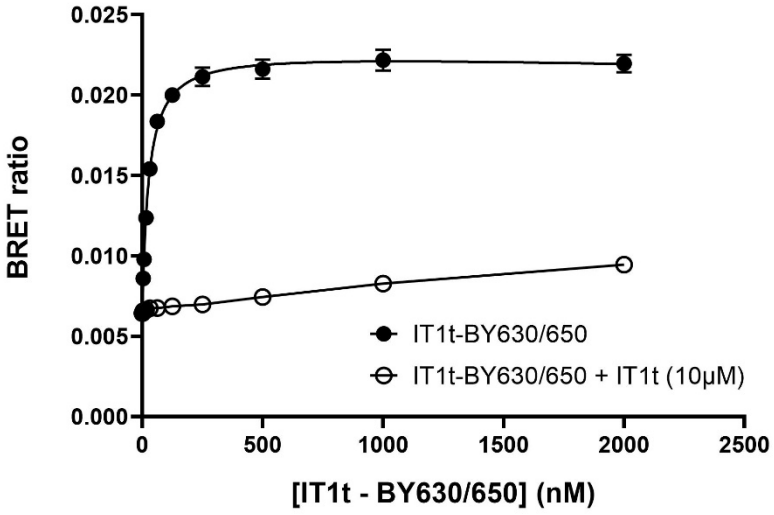

Fig S7: Determination of the binding affinity of IT1t-BY630/650 at NLuc/CXCR4 in HEK293 cells. (A) Chemical structure of IT1t-BY630/650. **(B)** NanoBRET saturation ligand binding curves obtained in HEK293 cells expressing genome-edited NLuc/CXCR4. Cells were incubated with increasing concentrations of IT1t-BY630/650 in the absence or presence of IT1t. Data shown represent mean ± SEM of N=5 independent experiments

Fig S8:

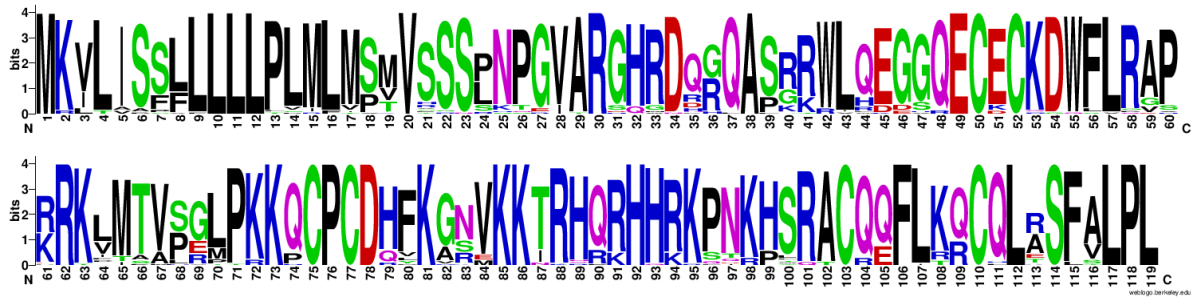

Fig S8: Conservation analysis of CXCL17. 'Sequence logo' generated for CXCL17 based on the multiple sequence alignment of forty-five 119 amino acid CXCL17 orthologues (table S1). Logo was generated using WebLogo[55]. Putative GAG binding sites between amino acids 85-101 appear highly conserved. See Fig 5A for putative GAG domains.

Fig S9

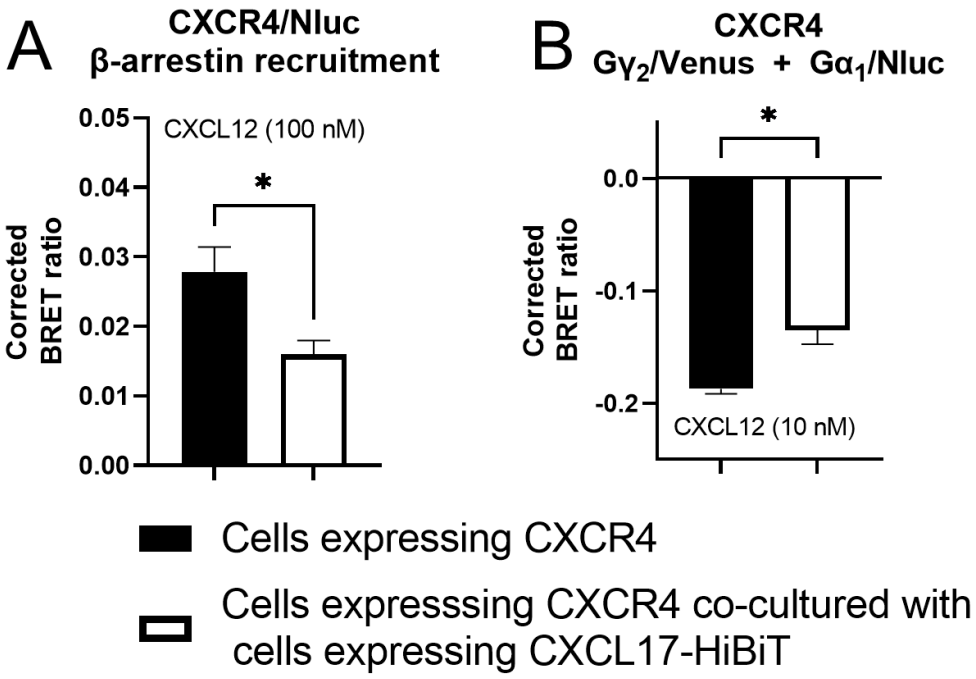

Fig S9: Fusion of HiBiT to the C-terminus of CXCL17 results in a functional protein that inhibits downstream CXCR4 signalling. HEK293 cells transiently transfected with CXCR4/Nluc and β-arrestin2/Venus (**A**) or CXCR4, $G\alpha_{i1}$/NLuc and Venus/$G\gamma_2$ (**B**) were co-cultured with wildtype HEK293 cells or HEK293 cells stably expressing CXCL17-HiBiT. Cells were stimulated with CXCL12 and BRET observed. Bars represent mean ± s.e.m. of N=3 **(A)** and N=3, **(B)** individual experiments.*, $p<0.05$, calculated by t-test.

Fig S10

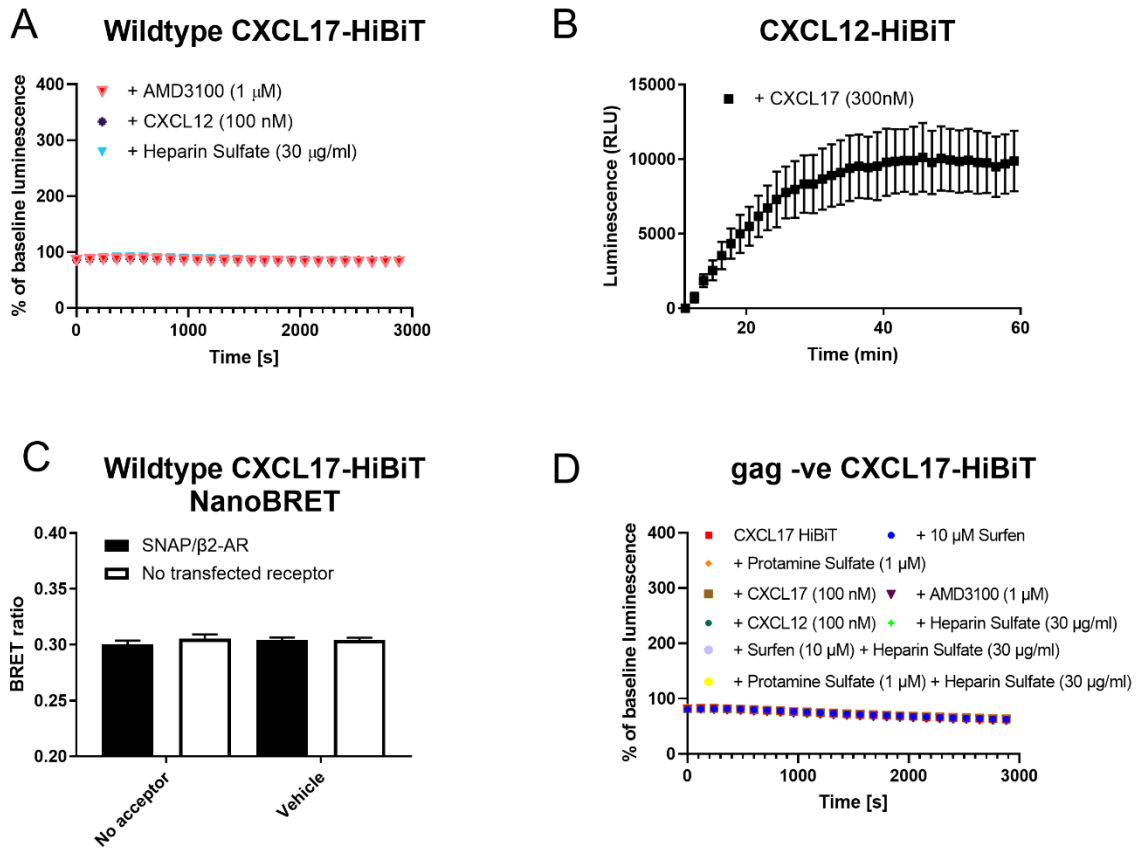

Fig S10: CXCL17 interacts with glycosaminoglycans via putative GAG binding domains. Related to Fig 6. (A) HEK293 cells transfected with CXCL17-HiBiT were treated with AMD3100, CXCL12 or heparin sulfate measured. **(B)** HEK293 cells expressing genome-edited CXCL12-HiBiT were treated with CXCL17 and luminescence measured. **(C)** HEK293 cells stably expressing CXCL17-HiBiT were transfected with SNAP/β2-ARand BRET measured. (**D)** HEK293 cells transfected with mutant CXCL17-HiBiT (gag -ve) were treated with AMD3100 , CXCL12 , CXCL17 , heparin sulfateor, surfen or protamine sulfate with or without heparin sulfate and luminescence measured. Points or bars represent mean ± s.e.m. of N=4 **(C)** or N=5, **(A)** N=5, **(B)** and N=5 **(D)** individual experiments. Data in **(A and D)** are summarised in Fig 6C, where the endpoint luminescence values are plotted as a histogram.

Table S1: DNA sequences of wildtype and mutant GAG binding deficient CXCL17-HiBiT.

	Sequence
Wildtype CXCL17-HiBiT	**GCCACC**ATGAAAGTATTGATTTCCAGTTTGCTCTTGTTGCTGCCTCTTATGTTGATGTCTATGGTGTCTTCTA GCTTGAATCCCGGGGTTGCAAGAGGTCATAGAGATCGCGGTCAAGCAAGCAGACGGTGGCTGCAGGAGGG GGGCCAGGAATGTGAATGCAAAGACTGGTTTTTGAGAGCACCTCGCAGAAAATTCATGACTGTGTCTGGCC TCCCCAAGAAACAGTGTCCGTGCGATCACTTCAAGGGAAACGTAAAAAAAACCCGACATCAAAGGCACCA TCGCAAGCCTAATAAACATTCACGCGCATGTCAGCAATTCTTGAAACAATGTCAGTTGCGCTCATTCGCTCT GCCCTTGGGTTCTAGCGGGGTGAGTGGGTGGCGATTGTTCAAGAAAATTTCATAA
Mutant GAG binding deficient CXCL17-HiBiT	**GCCACC**ATGAAAGTATTGATTTCCAGTTTGCTCTTGTTGCTGCCTCTTATGTTGATGTCTATGGTGTCTTCTA GCTTGAATCCCGGGGTTGCAAGAGGTGCAGCTGATGCAGGTCAAGCAAGCAGACGGTGGCTGCAGGAGGG GGGCCAGGAATGTGAATGCAAAGACTGGTTTTTGAGAGCACCTCGCAGAAAATTCATGACTGTGTCTGGCC TCCCCAAGAAACAGTGTCCGTGCGATCACTTCAAGGGAAACGTAGCTGCAACCGCTCATCAAGCGGCTCAT GCAAAGCCTAATGCTGCTTCAGCCGCATGTCAGCAATTCTTGAAACAATGTCAGTTGCGCTCATTCGCTCTG CCCTTGGGTTCTAGCGGGGTGAGTGGGTGGCGATTGTTCAAGAAAATTTCATAA

GCCACC; Kozak sequence.

ATGAAAGTAT…; hCXCL17

GGTTCTAGCGGG; GSSG linker

GTGAGTGGGT…; HiBiT

Table S2: CXCL17 orthologues used for conservation analysis

UniProt ID	Species
Q6UXB2	Homo sapiens (Human)
Q5UW37	Mus musculus (Mouse)
H2QGG7	Pan troglodytes (Chimpanzee)
H2NZ12	Pongo abelii (Sumatran orangutan) (Pongo pygmaeus abelii)
D4A875	Rattus norvegicus (Rat)
G1RII2	Nomascus leucogenys (Northern white-cheeked gibbon) (Hylobates leucogenys)
A0A2R8Z5Y3	Pan paniscus (Pygmy chimpanzee) (Bonobo)
A0A337SWE4	Felis catus (Cat) (Felis silvestris catus)
A0A2K6L964	Rhinopithecus bieti (Black snub-nosed monkey) (Pygathrix bieti)
A0A1U7R423	Mesocricetus auratus (Golden hamster)
E2R9V6	Canis lupus familiaris (Dog) (Canis familiaris)
A0A2K6ERT1	Propithecus coquereli (Coquerel's sifaka) (Propithecus verreauxi coquereli)
A0A2K6TQQ2	Saimiri boliviensis boliviensis (Bolivian squirrel monkey)
A0A2K5QSN6	Cebus capucinus imitator
G3QEQ3	Gorilla gorilla gorilla (Western lowland gorilla)
G1LEE3	Ailuropoda melanoleuca (Giant panda)
A0A0D9S176	Chlorocebus sabaeus (Green monkey) (Cercopithecus sabaeus)
A0A0A0MWN4	Papio anubis (Olive baboon)
A0A2K6PII8	Rhinopithecus roxellana (Golden snub-nosed monkey) (Pygathrix roxellana)
A0A2K6CE26	Macaca nemestrina (Pig-tailed macaque)
A0A2K5J518	Colobus angolensis palliatus (Peters' Angolan colobus)
A0A2K5EJ57	Aotus nancymaae (Ma's night monkey)
A0A2K5NDE8	Cercocebus atys (Sooty mangabey) (Cercocebus torquatus atys)
A0A2K5YG25	Mandrillus leucophaeus (Drill) (Papio leucophaeus)
F7DM35	Callithrix jacchus (White-tufted-ear marmoset)
G7PXR6	Macaca fascicularis (Crab-eating macaque) (Cynomolgus monkey)
K7GSG9	Sus scrofa (Pig)
A0A452FVG1	Capra hircus (Goat)
A0A2U3WHI5	Odobenus rosmarus divergens (Pacific walrus)
A0A383YZ12	Balaenoptera acutorostrata scammoni (North Pacific minke whale)
A0A340XH93	Lipotes vexillifer (Yangtze river dolphin)
A0A3Q7MES7	Callorhinus ursinus (Northern fur seal)
A0A2Y9TBG3	Physeter macrocephalus (Sperm whale) (Physeter catodon)

A0A2Y9HKW8	Neomonachus schauinslandi (Hawaiian monk seal) (Monachus schauinslandi)
A0A341DBJ7	Neophocaena asiaeorientalis asiaeorientalis (Yangtze finless porpoise)
A0A384DLG4	Ursus maritimus (Polar bear) (Thalarctos maritimus)
A0A3Q7VJ80	Ursus arctos horribilis
A0A0P6J2P1	Heterocephalus glaber (Naked mole rat)
A0A1S3ACN0	Erinaceus europaeus (Western European hedgehog)
A0A091EE70	Fukomys damarensis (Damaraland mole rat) (Cryptomys damarensis)
A0A2K5VQK7	Macaca fascicularis (Crab-eating macaque) (Cynomolgus monkey)
A0A2Y9L467	Enhydra lutris kenyoni
A0A485MDS2	Lynx pardinus (Iberian lynx) (Felis pardina)
F7EWH0	Macaca mulatta (Rhesus macaque)
K9IY53	Desmodus rotundus (Vampire bat)

Data obtained from Uniprot[56] and limited to 119 amino acid CXCL17 orthologues.

Table S3: Gains and filter setting used for data collection

Fig	Filter	Gain
Fig 1A	535-30 / 475-30	3600/3500
Fig 1B	535-30 / 475-30	3600/3500
Fig 1C	535-30 / 475-30	3000/2600
Fig 2A, B, and D	535-30 / 475-30	3600/3200
Fig 2C	535-30 / 475-30	3400/2400
Fig 3A, B, and G	610-LP / 460-80	2600/1900
Fig 3D	610-LP / 460-80	3200 / 1800
Fig 3E	610-LP / 460-80	3800 / 2200
Fig 3F	610-LP / 460-80	3600/3200
Fig 4	535-30 / 475-30	3600/3200
Fig 5B, C, and E	610-LP / 460-80	3600/3200
Fig 5D	610-LP / 460-80	3800/2200
Fig 6B, C, and E	Total luminescence	2400
Fig 6D	535-30 / 475-30	3600/3200
Fig 7A, and B	610-LP / 460-80	3200 / 1800
Fig 7c	535-30 / 475-30	3600/3200
fig S1C	535-30 / 475-30	3400/2800
fig S1B	535-30 / 475-30	3600/3500
fig S1C	535-30 / 475-30	3600/3500
fig S2	535-30 / 475-30	3600/3500
fig S3	535-30 / 475-30	3600/3500
fig S4A	610-LP / 460-80	3000/2400
fig S4B	610-LP / 460-80	3600/3200
fig S5A	Total luminescence	2800
fig S5B	610-LP / 460-80	3600/3200
fig S6A	610-LP / 460-80	3600/3200
fig S6B	610-LP / 460-80	3600/3200
fig S6C	610-LP / 460-80	3600/3200
fig S7B	610-LP / 460-80	3600/3200
fig S9	535-30 / 475-30	3600/3200
fig 10A and D	Total luminescence	2400
fig10B	Total luminescence	3600
fig S10C	535-30 / 475-30	3600/3200